J. Earth Syst. Sci. (2020)129 26
https://doi.org/10.1007/s12040-019-1269-4

Geochemistry of ultramafic–mafic rocks of Mesoarchean Sargur Group, western Dharwar craton, India: Implications for their petrogenesis and tectonic setting

Kiranmala Patra[1], R Anand[1,*], S Balakrishnan[2] and Jitendra K Dash[2]

[1]*Department of Applied Geology, Indian Institute of Technology (Indian School of Mines), Dhanbad 826 004, India.*
[2]*Department of Earth Sciences, Pondicherry University, Puducherry 605 014, India.*
**Corresponding author. e-mail: anandrajagopal78@gmail.com*

MS received 13 June 2018; revised 15 July 2019; accepted 18 July 2019

The Nuggihalli and Holenarsipur greenstone belts of the western Dharwar craton expose ultramafic–mafic rocks of the Mesoarchean. The rocks in these belts are geochemically considered as komatiites and komatiitic basalts with minor occurrences of tholeiitic and calc-alkaline basalts. The dominant ultramafic rocks of the Nuggihalli greenstone belt are layered and indicate fractionation processes at relatively shallower crustal levels. The Al-undepleted and Al-depleted signatures obtained could be attributed to magmatic differentiation processes and might be due to fractional crystallization of minerals such as hornblende and plagioclase, in addition to cumulus olivine and pyroxene. The chemical heterogeneity in the rocks of these greenstone belts might have therefore developed during the intrusion of the parental melts and their differentiation into a layered igneous complex. The differences in the lithological characteristics of the Holenarsipur and Nuggihalli greenstone belts can be explained by their different crustal levels of exposure. Presence of spinifex-textured komatiites need not necessarily imply that the sources have to be ultramafic and therefore of a deeper origin. This study indicates that the parental melts for unambiguous layered intrusive ultramafic–mafic complexes could be high-Mg basalts originating from relatively shallower levels. The probable geodynamic setting for the emplacement of the rocks of the two greenstone belts could be in a plume-modified mid-ocean ridge that was too thick and buoyant to be subducted, and the decompression-melted magma chamber developed igneous layering as the magma stalled in the lithosphere.

Keywords. Dharwar craton; Sargur Group; Mesoarchean; Ridge subduction.

1. Introduction

Mafic–ultramafic rocks provide window to understand composition of mantle sources and pressure and temperature conditions of melting (Herzberg and Zhang 1996; Falloon *et al.* 2008). Peridotites, spinifex-textured komatiites, komatiitic basalts and minor tholeiitic rocks generally occur in association in many Archean greenstone belts distributed in different cratons (Schau 1977; Groves *et al.* 1984; Arndt and Jenner 1986; Compston *et al.* 1986; Storey *et al.* 1991; de Wit *et al.* 1992; Lesher and Arndt 1995; Arndt *et al.* 1997; Hollings *et al.* 1999; Arndt 2008; Kroner *et al.* 2016; Sossi *et al.* 2016). Inferring the source for the generation of compositionally distinct rocks such as above requires a detailed understanding of the nature of the mantle, depth of melt generation, degree of melting, Archean geotherms, and extent of crust-mantle interaction. Different tectonic settings were

Published online: 20 December 2019

suggested for emplacement of these magmatic rocks by various studies. Restricted occurrence of komatiites and komatiitic basalts during the Archean and their near complete absence in the Phanerozoic, makes it even more enigmatic to understand mantle dynamics and thermal regime responsible for generation of these ultramafic magmas. However, many studies point towards komatiitic magmas derived from plumes originating from the lower mantle (Ohtani *et al.* 1989; Ohtani 1990; Jochum *et al.* 1991; Herzberg 1992; Saunders *et al.* 1996; Lahaye *et al.* 1995; Kerr *et al.* 1995, 1996; Abbott 1996; Herzberg and Zhang 1996; Arndt *et al.* 1997; Fitton *et al.* 1997; Polat *et al.* 1998; Herzberg 1999; Hollings *et al.* 1999; Kerrich *et al.* 1999; Puchtel *et al.* 1999; Polat *et al.* 1999; Polat and Kerrich 2000; Revillon *et al.* 2000; Anhaeusser 2001; Kerrich and Xie 2002; Grove and Parman 2004; Jayananda *et al.* 2008; Pearce 2008; Zhang *et al.* 2009; Robin-Popieul *et al.* 2012; Nebel *et al.* 2013; Wyman and Hollings 2015; Sobolev *et al.* 2016). Arndt *et al.* (1997) discounted fractional crystallization and partial melting alone for the observed variations in the REE concentrations of the basalts and komatiites of Gorgona and advocated dynamic melting in a heterogeneous mantle source. Elliott *et al.* (1991) and Maya *et al.* (2016) also inferred dynamic melting wherein the melts were produced at different depths from a rising plume of a predominantly peridotitic mantle.

Many of the Archean ultramafic–mafic suites of rocks are known to have a depleted source characteristic of MORB and also show depletion in certain high field strength elements (HFSE) similar to those observed in subduction-zone magmas (Jochum *et al.* 1991; Abbott 1996; Hollings *et al.* 1999; Chavagnac 2004; Pearce 2008; Robin-Popieul *et al.* 2012; Wyman and Hollings 2015). This mixed characteristics and the absence of an enriched trace element signature normally observed in plume-related magmas as in the ocean islands (OIB) needs better explanation.

Layered intrusive complexes consisting of intrusive dunite, peridotite, pyroxenite, gabbro and anorthosite associated with extrusive komatiite and pillowed basalts are reported from many Paleoarchean and Mesoarchean greenstone belts (Arndt and Jenner 1986; Lahaye *et al.* 1995; Kerr *et al.* 1996; Saunders *et al.* 1996; Jayananda *et al.* 2008; Zhang *et al.* 2009; Mukherjee *et al.* 2010, 2012; Nebel *et al.* 2013; Sappin *et al.* 2016). Instances of well-preserved oceanic crust in the form of layered mafic intrusions have been reported from most of the Archean cratons (Drury *et al.* 1984; Jayananda *et al.* 2008; Zhang *et al.* 2009; Mukherjee *et al.* 2010, 2012; Nebel *et al.* 2013; Sappin *et al.* 2016; Zhou *et al.* 2016; Polat *et al.* 2018). As development of layering is due to fractional crystallization, which, compared to depths at which melting and magma generation occur, is essentially a shallower depth/lower pressure process, elemental abundances of different rock units of a layered complex might merely be due to complementary enrichment and depletion brought about by differentiation processes. A detailed study of Archean layered intrusive complexes is necessary to understand their mode of formation and association with greenstone belts. Such complexes in the western Dharwar craton (WDC) are associated with komatiites in some of the greenstone belts and studies on the intrusive and extrusive ultramafic rocks of the Archean Sargur Group indicate their sources to be of deeper origin (Jayananda *et al.* 2008; Maya *et al.* 2016). However, the presence of high-Mg minerals such as olivine, or their altered products, need not necessarily indicate that the parental melts have to be high temperature komatiitic melts (Keiding *et al.* 2011). Keiding *et al.* (2011) also noted that high-Mg minerals in ultramafic melts might also result from Fe depletion of a mantle column undergoing dynamic melting and inferred a basaltic source for the Paraná-Etendeka large igneous province from Namibia, based on studies on melt inclusions. Further, Herzberg and O'Hara (2002) have described the formation of high-Mg olivine from advanced fractional melts, due to reduction in the FeO content of the magma during decompression from a higher pressure.

The depth of the genesis of the source magmas, the degree of melting involved in the generation of magmas, the style of plate tectonics during Archean and the extent of interaction with older lithosphere require to be understood in better light. The Mesoarchean Sargur Group of rocks in the WDC are represented by several greenstone belts, some of which have been recognized as layered mafic–ultramafic intrusive complexes exposed as linear belts, while others are dismembered units present as enclaves tucked within the vast expanse of tonalite–trondhjemite–granodiorite (TTG) gneisses, distributed widely across the craton (Chadwick *et al.* 1985a, b, 1989; Srikantappa *et al.* 1985; Radhakrishna and Naqvi 1986; Drury *et al.* 1987; Meen *et al.* 1992; Nutman *et al.* 1992, 1996; Peucat *et al.* 1993, 1995;

Ramakrishnan *et al.* 1994; Rogers 1996; Radhakrishna and Vaidyanadhan 1997; Trendall *et al.* 1997a, b; Bhaskar Rao *et al.* 2000; Naqvi 2005; Naqvi and Prathap 2007; Jayananda *et al.* 2006, 2008; Mukherjee *et al.* 2010, 2012). The rocks of the intrusive/extrusive complexes are also found associated with komatiitic flows, recognized by their prominent spinifex texture, as well as, pillowed basalts (Viswanatha *et al.* 1977; Jafri *et al.* 1997; Swami Nath and Ramakrishnan 1981; Bidyananda *et al.* 2003; Jayananda *et al.* 2008; Mukherjee *et al.* 2010, 2012; Tushipokla and Jayananda 2013; Maya *et al.* 2016). The presence of a sialic basement for the emplacement of the mafic–ultramafic rock units has been suggested because of the occurrence of gneisses older than the Sargur supracrustal rocks in Gorur area west of Holenarsipur greenstone belt, whereas, Sargur rocks occurring as dismembered units in the southern part of the Dharwar craton were interpreted as older than TTG gneisses (Beckinsale *et al.* 1980, 1982; Naqvi 1981; Ramakrishnan and Viswanatha 1981; Hussain and Naqvi 1983; Monrad 1983; Taylor *et al.* 1984; Peucat *et al.* 1989, 1993, 1995; Bhaskar Rao *et al.* 1991, 2000; Meen *et al.* 1992; Nutman *et al.* 1992; Naha *et al.* 1993). The similarity in the development of the metamorphic fabric in mafic–ultramafic rocks, as well as, the adjacent TTG gneisses precludes unequivocal establishment of temporal relationship between these rock units. However, several phases of granitic magmatic activities have been reported indicating multiple settings and different times for the emplacement of and interaction between mafic and felsic sources (Naqvi and Hussain 1973; Bhaskar Rao and Naqvi 1978; Naqvi *et al.* 1978, 2002, 2006; Ananta Iyer and Vasudev 1979; Drury 1981, 1982, 1983; Swami Nath and Ramakrishnan 1981; Bhaskar Rao and Drury 1982; Naqvi and Rogers 1987; Peucat *et al.* 1987, 1989, 1993; Manikyamba and Naqvi 1997). The excellent preservation of layered sequences in the larger linear ultramafic–mafic greenstone belts, particularly in the Nuggihalli belt, unlike the smaller enclave suites, may hold important clues to decipher tectonic setting and petrogenetic evolution of these rocks. In this work, detailed geochemical study has been carried out on the metamorphosed ultramafic–mafic rocks of the Nuggihalli and Holenarsipur greenstone belts for attempting to propose a model for the petrogenesis of their igneous protoliths and their tectonomagmatic evolution.

2. Regional geological setting

The Archean Dharwar craton (figure 1a) is divided into eastern and western blocks based on the distinctive features observed in the rocks of the greenstone-granite terranes exposed on either side of the eastern margin of the Chitradurga greenstone belt and degree of regional metamorphism (Swami Nath *et al.* 1976; Rollinson *et al.* 1981; Meen *et al.* 1992; Nutman *et al.* 1992, 1996; Peucat *et al.* 1993; Jayananda *et al.* 2008, 2013; Sarma *et al.* 2011; Tushipokla and Jayananda 2013).The western Dharwar craton (WDC) is generally considered to be composed of two generations of greenstone magmatism. The older Sargur greenstone belts and the younger Dharwar-type greenstone belts are considered to be separated in time by the extensive TTG gneisses (Chadwick *et al.* 2000; Jayananda *et al.* 2000, 2006, 2008; Chardon *et al.* 2011; Hokada *et al.* 2012; Tushipokla and Jayananda 2013). Alternatively, the Sargur group rocks have also been considered by some researchers to be higher grade metamorphic equivalents of the Dharwar Supergroup (Srinivasan 1988; Naha *et al.* 1991; Das Sharma *et al.* 1994). The rocks of the Sargur Group occur either as linear mafic–ultramafic belts that progressively narrow down and get dismembered into enclaves within TTG gneisses towards the south. The contact between the TTG gneisses and the overlying Dharwar supergroup rocks is marked by a distinct polymictic conglomerate. Such relations have not been established for Sargur group of rocks. The larger narrow belts are made up of layered intrusive rocks of ultramafic and mafic composition, while the dismembered enclave suites that are much smaller in their dimensions are not recognizably layered. The rocks of the Sargur Group are exposed at several localities that include Holenarasipur, Nuggihalli, Nagamangala, Kalyadi, Aldahalli, Krishnarajpet, J.C. Pura, Banasandra, Hadnur, Ghattihosahalli and the type locality, Sargur (Naqvi 1981). The rocks of the Sargur Group are predominantly ultramafic–mafic in composition and are composed of peridotite, pyroxenite, hornblendite, dunite and serpentinized ultramafic rocks (Viswanatha *et al.* 1977; Chadwick *et al.* 1981; Swami Nath and Ramakrishnan 1981; Srikantia and Venkataramana 1989; Srikantia and Rao 1990). All these rocks have been variably metamorphosed to differing grades as there is a general increase in metamorphic grade from north towards south in the Dharwar craton

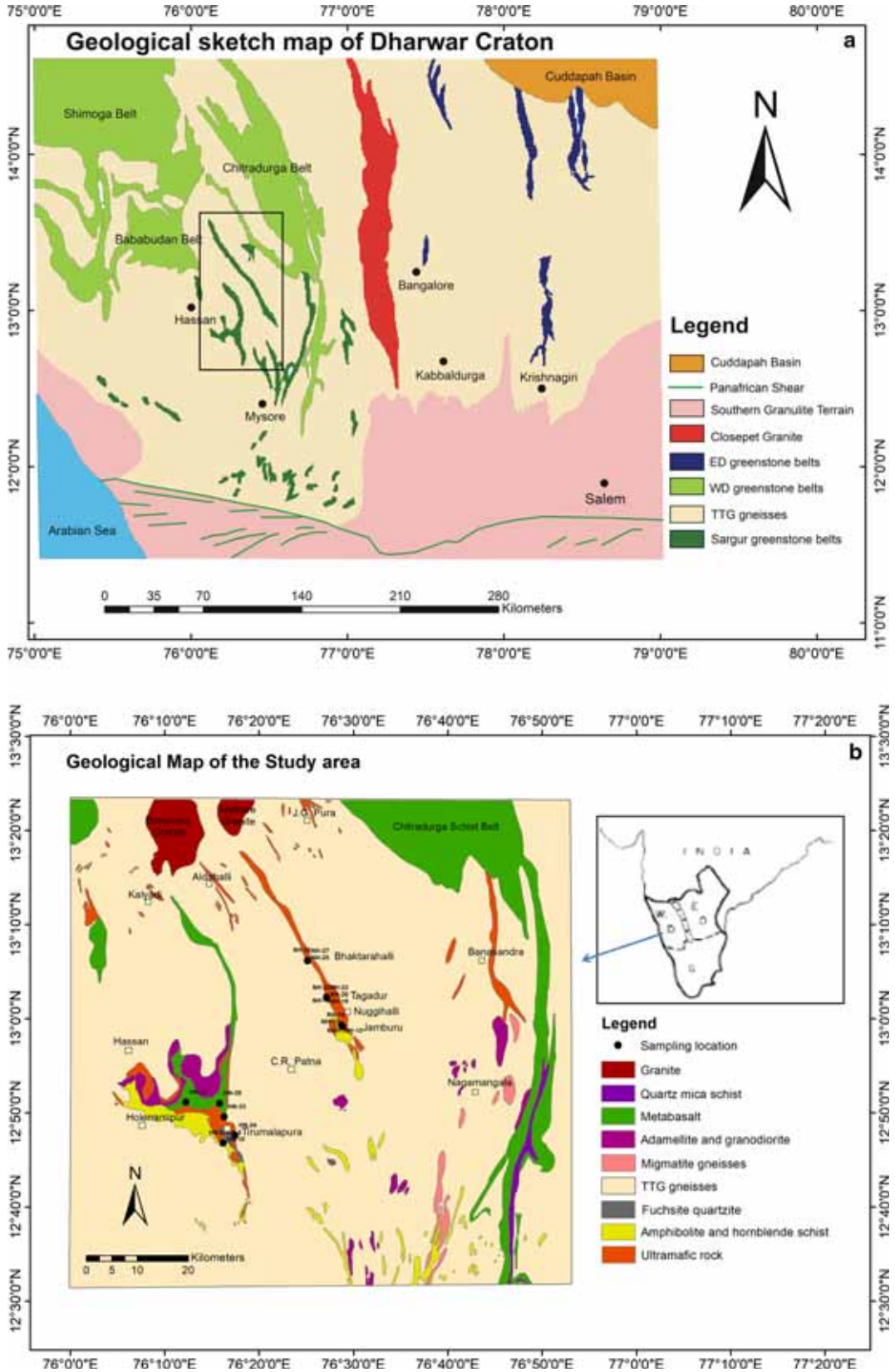

Figure 1. (**a**) Geological map of the Dharwar craton showing the different greenstone belts (after Chardon *et al.* 2002). (**b**) Geological map showing the Holenarsipur and Nuggihalli greenstone belts with sample locations (digitized from Geological Quadrangle Maps 57C, 1997 and 57D, 2008, Geological Survey of India).

(Srikantappa *et al.* 1985). The grade varies from middle to upper amphibolite grade in the north up to granulite grade in the type area (Srikantappa *et al.* 1985; Peucat *et al.* 1995; Bhaskar Rao *et al.* 2000). The general composition of the ultramafic–mafic assemblages has been determined to be komatiitic and tholeiitic and several reports of spinifex-textured komatiites and pillowed basalts of tholeiitic composition exist (Balakrishnan *et al.* 1990; Bhaskar Rao *et al.* 1992; Zachariah *et al.* 1995; Kumar *et al.* 1996; Nutman *et al.* 1996; Naqvi *et al.* 2002; Manikyamba *et al.* 2005). The rocks of the larger greenstone belts of Sargur Group such as Nuggihalli and J.C. Pura are dominantly made up of intrusive peridotites that are often found to be serpentinized, and metabasalts and the volcanic komatiites and basalts are largely insignificant. South of Mysore, the rocks are metamorphosed to granulite facies at about 2.5 Ga ago (Buhl *et al.* 1983; Srikantappa *et al.* 1985) which could represent deeper part of continental crust (Chardon *et al.* 2002).

2.1 *Holenarsipur greenstone belt (HGB)*

The Holenarsipur belt is roughly trident-shaped, deflected around granites in the north and pinched-out as a narrow belt within the gneisses in the south (figure 1b) (Swami Nath and Ramakrishnan 1981; Bhaskar Rao *et al.* 2000). The dominant rock types of the belt include metasediments such as kyanite-staurolite-garnet-mica-graphite pelitic schists, serpentinized ultramafic intrusive rocks, amphibolites, peridotite-gabbro-anorthosite sequences, talc-tremolite-chlorite-actinolite schists, metaquartzites and banded iron formations. Minor occurrences of spinifex-textured komatiites are also reported from the northern part of the belt (Jafri *et al.* 1997; Bhaskar Rao *et al.* 2000). The belt has been variably interpreted as consisting of both the Sargur-type and Dharwar-type supracrustal rocks by some authors, while others interpret the greenstone sequences as belonging to only the Sargur-type stratigraphy (Srinivasan 1988; Naha *et al.* 1991; Das Sharma *et al.* 1994). Excellent exposures of the schistose ultramafic rocks with a clearly intrusive gabbro unit are found in the Tirumalapura hill near Holenarsipur, thanks to the road cut recently for the temple on top of the hill. The foliation developed in the schistose rocks does not continue into the intrusive rocks. Minor development of weathered anorthositic rocks is also found which could be a part of the older foliated sequence. The amphiboles are more altered in the host schist than in the intrusive gabbro. A conglomerate horizon is thought to be the boundary between the juxtaposed Sargur Group supracrustal rocks and the younger Dharwar Group supracrustal rocks (Viswanatha and Ramakrishnan 1975; Chadwick *et al.* 1978; Swami Nath and Ramakrishnan 1981). On the contrary, Naqvi *et al.* (1978) interpreted these conglomerates as intraformational rather than unconformity-related ones, which was supported by Srinivasan (1988) who observed the lithological differences on either side of the conglomerate horizon as a result of variations in sedimentological and volcanic development of a single volcano-sedimentary sequence. While the rocks south of the conglomerate horizon are predominantly metasedimentary, amphibolite and ultramafic intrusive rocks, those north of the conglomerates are typically metabasalts, often amygdular, quartzites and iron formations. Sparse geochronological information available does not divide these two set of formations as distinct units separated in time (Drury *et al.* 1987; Kunugiza *et al.* 1996; Bhaskar Rao *et al.* 2000). Bouhallier *et al.* (1993) did a detailed structural study of the rocks of the HGB and concluded that the entire sequence from north to south had undergone the same tectono-metamorphic history and that the primary deformation fabric developed during the 3.1–3.0 Ga intrusions of TTG gneisses. The strain trajectories were interpreted to have developed due to bulk deformation during the tectono-metamorphic event resulting in regional (NE–SW) shortening interfering with diapiric domes (Bouhallier *et al.* 1993). Bouhallier *et al.* (1993) also inferred elliptical dome and basin structures based on their detailed structural mapping of the greenstone-granite terrane. Peucat *et al.* (1995) have reported a 3298 ± 7 Ma zircon age for a metarhyolite in the HGB. The gneissic samples of Holenarsipur area have given ages in the range of 3.1–3.3 Ga (Bidyananda *et al.* 2003) and the gneissic rocks are considered to be nearly contemporaneous with the adjacent metasediments. Bhaskar Rao *et al.* (2000) have obtained Sm–Nd ages of 3.285 Ga for Honnavalli meta-anorthosite and 2.495 Ga for Dodkadnur meta-anorthosite, the latter age they attribute to isotopic re-equilibration during the Neoarchean 2.5 Ga tectonothermal event.

Representative samples of actinolite schists and plagioclase-rich rocks were collected from several localities in the Holenarsipur area as indicated in

figure 1b for detailed petrographic and geochemical study.

2.2 *Nuggihalli greenstone belt (NGB)*

The Nuggihalli belt is a linear ultramafic belt extending for about 50 km with a NNW–SSE trend (figure 1b). This belt is well known primarily for the occurrence of several economically significant chromite as well as vanadiferous–titaniferous magnetite deposits hosted by ultramafic–mafic rock association. Amphibolite, pillowed tholeiitic and spinifex-textured komatiitic rocks, serpentinized peridotite, gabbro, anorthosite, chromitite as well as schistose rocks such as hornblende schist, garnet-biotite schist, kyanite-mica schist and tremolite-actinolite-chlorite-quartz schist comprise the ultramafic–mafic rock sequence. Spinifex-textured komatiite, though minor, occurs in the northern part of the belt near Bhaktarahalli (Jafri *et al.* 1997). Several working and abandoned mines for chromite and V-Ti-magnetites expose vast units of ultramafic rocks that show layering, indicating an intrusive emplacement followed by fractional crystallization, and different degrees of serpentinization. The chromite mine in Tagadur has a variety of rock types that have been metamorphosed including serpentinized dunite/peridotite, tremolite–actinolite–chlorite schist, metapyroxenite, gabbro, amphibolite and anorthosite. Rapid magmatic differentiation or tectonic interleaving is considered as the possible mechanism for the development of thin layers of rocks of the differentiation sequence (Swami Nath and Ramakrishnan 1981). Amphibolites are both schistose and massive representing singular intrusions of mafic sills and layered intrusion, respectively (Swami Nath and Ramakrishnan 1981; Mukherjee *et al.* 2010, 2012). The chromite mine in Jamburu also exhibits similar rock types as in Tagadur. The general trend of the foliation parallels the NNW–SSE trend of the belt with minor folds developed on the chromitite layers. No development of interfering foliations is observed in the belt and dome and basin structures observed in the HGB are conspicuously absent in the NGB. The peridotitic rocks of NGB have given a Sm–Nd age of 3125 ± 120 Ma (Mukherjee *et al.* 2012). Jayananda *et al.* (2008) have reported a 3352 ± 110 Ma Sm–Nd age for the komatiitic rocks by including samples from J.C. Pura Banasandra, Nuggihalli, Kalyadi and Ghattihosahalli. Whereas, Maya *et al.* (2016) reported a Sm–Nd isochron age of 3137 ± 190 Ma for komatiites of Banasandra. Patra *et al.* (2016) have obtained a younger Sm–Nd age of 2925 ± 68 Ma for the peridotitic rocks of NGB.

3. Sampling and petrography

Detailed field work was carried out mainly in Holenarsipur and Nuggihalli greenstone belts to understand the field disposition of the different lithologies in the belts. About 2–3 kg of representative samples were collected from least-altered outcrops of ultramafic and mafic rocks exposed at the Holenarsipur and Nuggihalli areas of Karnataka for petrographic and geochemical studies. Exposures of less altered ultramafic rocks are sparse in the Holenarsipur area. The Tirumalapura hill road cutting reveals excellent exposures of metamorphosed mafic–ultramafic intrusives ranging in composition from talc-tremolite schist, tremolite-actinolite schist through gabbro to anorthosite (figure 2a and b). The hill adjacent to the Tirumalapura road cutting exposes serpentinized peridotite exhibiting extensive serpentinization. The serpentinized ultramafic rocks were unsuitable for geochemical studies and therefore were not collected. A gabbro body is found intrusive into the talc-tremolite schist and shows good development of chilled-baked margins at the contact. Based on the field observations, this gabbro can be considered to be a later intrusive in the ultramafic sequence.

In the Nuggihalli area, existing and abandoned chromite mines in Tagadur, Jamburu and Bhaktarahalli expose well preserved complexes of ultramafic–mafic sequences consisting of talc-tremolite schist, serpenitinized dunite, peridotite, chloritized ultramafic rock, chromitite bands, metapyroxenite, metahornblendite, metagabbro and anorthosite (figure 2c, d, and e). These rocks are present as differentiated sills with anorthosites capping gabbro-peridotites at places. Minor amphibolites are also found in these mines. Individual layers could be identified by their mineral composition as distinct units of serpentized peridotite, pyroxenite, gabbro, anorthosite and titaniferous–vanadiferous magnetite exposed bottom-up in Tagadur chromite mines (figure 2e). These field observations are unambiguous evidence for igneous layering in the study area, particularly in NGB. The layering is by and large mineralogical and can

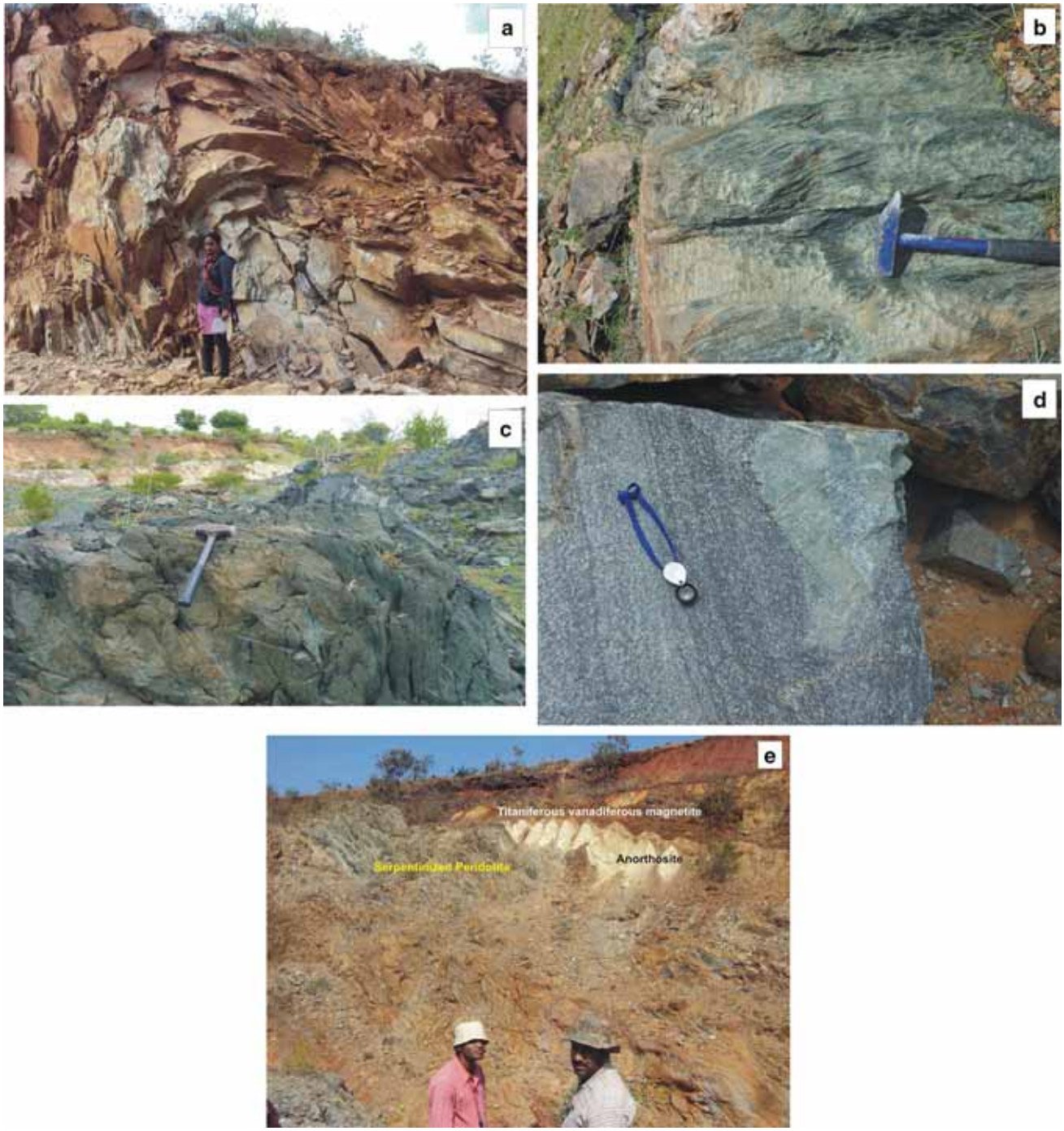

Figure 2. Field photograph of (**a**) folded talc tremolite schist associated with gabbro, exposed in Tirumalapura hill near Holenarsipur; (**b**) chlorite schist and (**c**) serpentinized peridotite exposed in the Tagadur mine, Nuggihalli; (**d**) ultramafic rock showing cumulus texture near Bhaktarahalli mine, Nuggihalli (**e**) layered intrusive structure of ultrabasic-basic rocks in Tagadur area of Nuggihalli greenstone belt.

be interpreted to be formed due to fractional crystallization based on the observed lithologies in the layered sequence.

Petrographic study of HGB samples show variation in terms of grain size, texture, mineralogy and degree of alteration. The samples HN-05 (figure 3a) and HN-27 are from the gabbro unit intruding the talc-tremolite schist in the Tirumalapura hill and are composed of abundant hornblende, actinolite, plagioclase, chlorite and minor quartz with titanite present as an accessory mineral. The gabbros do not show any schistosity. HN-10 (figure 3b) was collected from beside the Tirumalapura hill and is made up of hornblende,

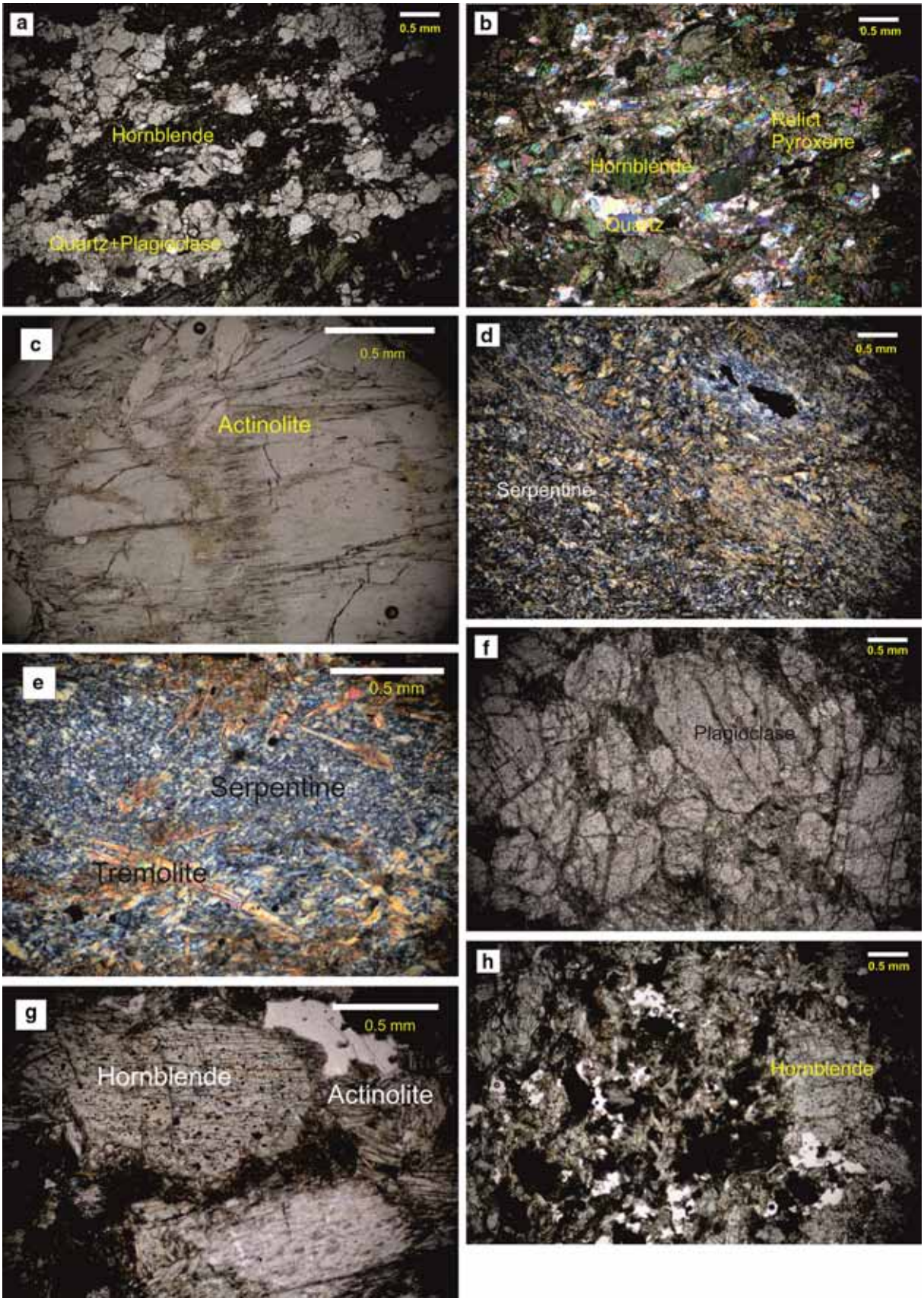
a
0.5 mm
Hornblende
Quartz+Plagioclase
b
0.5 mm
Relict
Pyroxene
Hornblende
Quartz
c
0.5 mm
Actinolite
d
0.5 mm
Serpentine
e
0.5 mm
Serpentine
Tremolite
f
0.5 mm
Plagioclase
g
0.5 mm
Hornblende
Actinolite
h
0.5 mm
Hornblende

◀Figure 3. Photomicrograph of (**a**) metagabbro (HN-05) showing abundant hornblende and plagioclase; (**b**) amphibolite showing relict pyroxene crystals (HN-10) from Tirumalapura hill near Holenarsipur; (**c**) amphibole-rich ultramafic rock collected from HGB (HN-33) near Kumkumna Hosuru village; (**d**) and (**e**) serpentinized dunite (NH-10 and NH-11) from Jamburu mine, Nuggihalli; (**f**) anorthositic rock (NH-12) from the layered igneous complex occurring in the Jamburu mine, Nuggihalli; (**g**) and (**h**) amphibolites of komatiitic basaltic composition (NH-22 and NH-20) collected from different benches of the Tagadur mine, Nuggihalli.

chlorite, plagioclase, tremolite, minor quartz and traces of relict pyroxene. Presence of relict primary mineral phases is indicative of crystallization from a mafic–ultramafic magma prior to their metamorphic recrystallization. Sample HN-24, collected from near Tevadahalli village, consists of abundant hornblende, tremolite, chlorite, anthophyllite with minor quartz. Two samples HN-28 and HN-33 (figure 3c), collected near Kumkumna Hosuru village, are chiefly made up of tremolite–actinolite, hornblende, chlorite, cummingtonite and ferrogedrite. The latter two minerals could be recognized by XRD analysis. These rocks exhibit elongated actinolite needles, ultramafic in composition and had suffered post-crystallization alteration. HN-31, a metabasalt from northern part of the HGB containing plagioclase, tremolite, biotite and quartz as major minerals (figure 1b), is different from rest of the samples of HGB. HGB rocks are mostly fine- to medium-grained showing inequigranular texture. In some rocks (metagabbro and amphibolite), most quartz grains are showing anhedral inequigranular mosaic texture which is an indication of recrystallization during the medium grade metamorphic alteration of the parental rocks.

The NGB is dominated by ultramafic intrusive rocks. Samples NH-10, NH-11, NH-12 (figure 3d, e, f) and NH-14 were collected from Jamburu chromite mine area of NGB. NH-10 and NH-11 are serpentinized ultramafic rocks that are fine-grained and are composed completely of antigorite, chlorite and tremolite. No primary mineralogy seems to be preserved in these rocks. However, carbonate mineral phases are completely absent in these metaperidotites. Textural evidence shows no significant development of foliation in these rocks in the thin section. Needles of tremolite lie embedded in a serpentinized matrix (figure 3e). NH-12 and NH-14 are from the upper benches of the Jamburu mine in which the former is made up of abundant plagioclase with minor amounts of actinolite and is petrographically identified as leucogabbro whose plagioclase grains are compositionally anorthite as confirmed by EPMA and XRD analyses. NH-14 is composed of plagioclase, hornblende, actinolite and minor quartz and is gabbroic in composition. The samples NH-16, 22 and 23 were collected from the lower benches of Tagadur chromite mine. While NH-16 is predominantly made up of chrysotile, lizardite, tremolite, chlorite and chromite, NH-22 (figure 3g) and 23 are actinolite–chlorite schists with no significant preservation of primary pyroxenes. From the upper benches of the mine in Tagadur samples NH-17, 18, 19 and 20 were collected. NH-20 (figure 3h) is composed of actinolite and chlorite; NH-19 is made of chrysotile, chlorite and actinolite; NH-18 is almost completely made up of actinolite. The schistose rocks are composed of lizardite-chromite, and talc-tremolite-hornblende, quartz-tremolite-hornblende and quartz-plagioclase-actinolite with opaque minerals. The ultramafic rocks of NGB have been subjected to varying degrees serpentinization and the primary mineralogy of the rocks of the greenstone belts studied is not preserved in any of them due to metamorphism of these rocks under mid-amphibolite facies conditions.

4. Analytical methods

Rock samples weighing 500 g to 1 kg were pulverized using a jaw crusher to 1 mm and 10 mm size. Samples were powdered using a tungsten carbide ring mill (at IIT, Kharagpur) and analysed for trace element analysis and Rare Earth Element (REE) analysis by ICPMS (Thermo Element-2) at Department of Earth Sciences, Pondicherry University, Puducherry. Approximately 500 mg of sample powders were dissolved in double distilled HF:HNO_3:HCl (7:3:1) mixture at 100°C for 1 day, then mixture was dried at 120°C temperature and the further attacked with double distilled concentrated HNO_3 for two times. After drying, double distilled concentrated HNO_3:HCl (3:1) mixture was added. Mixture was dried on hot plate for 2–3 days below 100°C temperature. Finally 5 ml 2N HCl was added until no residue was visible. The clear solution was diluted to required extent and used for trace element analysis using ICPMS. Rock standards AGV and BCR2 were used for checking the accuracy and precision of the measurements. Analytical errors were within permissible limits compared to the reported values of the reference

material. Major element (including LOI) analysis was carried out using an X-Ray Fluorescence (XRF) Spectrometer from the National Centre of Earth Science Studies (NCESS), Thiruvananthapuram, Kerala. Electron Probe Microscope Analysis (EPMA) was carried out from Central Research Facility (CRF) Lab, Indian Institute of Technology (Indian School of Mines), Dhanbad, Jharkhand. The analytical setting for the EPMA was an electron beam of 1–3 μm diameter, operated at 15 kV and 15 nA. The minerals used as standards were Albite for Na, Periclase for Mg, Almandine for Al and Si, Orthoclase for K, Apatite for Ca, Rutile for Ti, Cr_2O_3 for Cr, Rhodonite for Mn and Hematite for Fe. Powder X-Ray Diffraction (XRD) study was carried out at the Department of Earth Sciences, Pondicherry University, Puducherry.

5. Results

The mafic and ultramafic rocks of Sargur-affinity in the HGB and NGB show trends in the wt% major element oxides *vs.* Mg# [Mg# = 100(Mg/(Mg+Fe^{2+}))] plots (figure 4). Al_2O_3, CaO and TiO_2 show negative correlation with Mg#. Trends in the Na_2O and K_2O *vs.* Mg# plots indicate differentiation processes in the formation of mafic and ultramafic rocks (figure 4). No significant trends are observed in trace elements such as Nb, Zr, Nd and Yb *vs.* MgO (figure 5). Jensen's plot, primarily defined for volcanic rocks and modified by Viljoen and Viljoen (1982), has been considered for obtaining the approximate compositions of the ultramafic–mafic rock suites of NGB and HGB. The ultramafic rocks are compositional equivalents of komatiites and komatiitic basalts, while three of the samples can be considered as tholeiitic and one as calc-alkaline in composition (figure 6). The latter sample, NH-12, is a plagioclase-rich amphibolitic rock that was collected from the top benches of Jamburu chromite mines and has unambiguous association with the peridotitic rocks of NGB. The composition of the plagioclase has been determined using EPMA to be anorthite (An_{91}). Among the samples collected from different parts of the Holenarsipur belt, samples HN-24, HN-28 and HN-33 with MgO wt% of 19.59%, 23.13% and 20.65% respectively, and TiO_2 wt% 0.65%, 0.69% and 0.66% respectively, are komatiitic in composition, though no spinifex texture can be noticed in these rocks. The chondrite-normalized REE pattern for these rock samples shows significant LREE enrichment with negative Eu anomaly (figure 7a). The LREE in these samples are at least 10 times enriched relative to chondrite. The mafic sample HN-10 collected from the schistose rock units of the Tirumalapura hill also shows an LREE enriched pattern with negative Eu anomaly. The plagioclase-rich samples from the same hill (HN-05 and HN-27) found intruding the talc tremolite actinolite schists exhibit a near flat REE pattern with positive Eu anomaly (figure 7a). The REE contents of these samples are less enriched relative to chondrite and may indicate their origin from a source significantly different from the source of the schistose rocks. The $(La/Yb)_N$, $(La/Sm)_N$ and $(Gd/Yb)_N$ ratios for the samples HN-24, HN-28 and HN-33 range from 2.22 to 5.79, 1.63 to 3.88 and 1.91 to 2.16 respectively (table 1). The sample HN-31 collected from a location classified as part of the Bababudan (Srinivasan 1988), north of Holenarsipur, has a more fractionated REE pattern with $(La/Yb)_N$ ratio of 7.51 and $(Gd/Yb)_N$ ratio of 2.69.

The chondrite-normalized REE patterns for the Nuggihalli ultramafic samples are flat and near chondritic (figure 7b). The peridotitic samples (NH-10 and NH-11) from Jamburu chromite mines are LREE depleted with $(La/Yb)_N$, $(La/Sm)_N$ and $(Gd/Yb)_N$ ratios ranging from 0.40 to 0.70, 0.71–1.03 and 0.57–0.76, respectively (table 1). The peridotitic samples (NH-19, NH-20, NH-22 and NH-23) from Tagadur chromite mines too are LREE depleted with $(La/Yb)_N$, and $(La/Sm)_N$ ratios ranging from 0.43 to 0.86 and 0.36–0.78 (table 1) respectively, while their $(Gd/Yb)_N$ ratio ranges from 1.27 to 1.49 indicating a relatively more fractionated HREE with respect to MREE. One sample, NH-16 from the lower bench of the Tagadur chromite mines however, shows lower concentrations of REE with an LREE enriched chondrite-normalized pattern with $(La/Yb)_N$, and $(La/Sm)_N$ ratios of 2.09 and 1.48 respectively and a fractionated $(Gd/Yb)_N$ ratio of 1.57. All the above samples from Jamburu and Tagadur mines show negative Eu anomalies. Three samples of ultramafic layers from Bhaktarahalli mines (NH-25, NH-26 and NH-27) show positive Eu anomalies in their chondrite-normalized REE patterns with LREE enrichment (figure 7b). The $(La/Yb)_N$, $(La/Sm)_N$ and $(Gd/Yb)_N$ ratios for these samples range from 1.82 to 2.86, 1.61 to 2.18 and 0.88 to 1.22 respectively (table 1).

The mafic samples collected from Nuggihalli are showing super-chondritic concentration for most of the trace elements. The plagioclase-rich sample

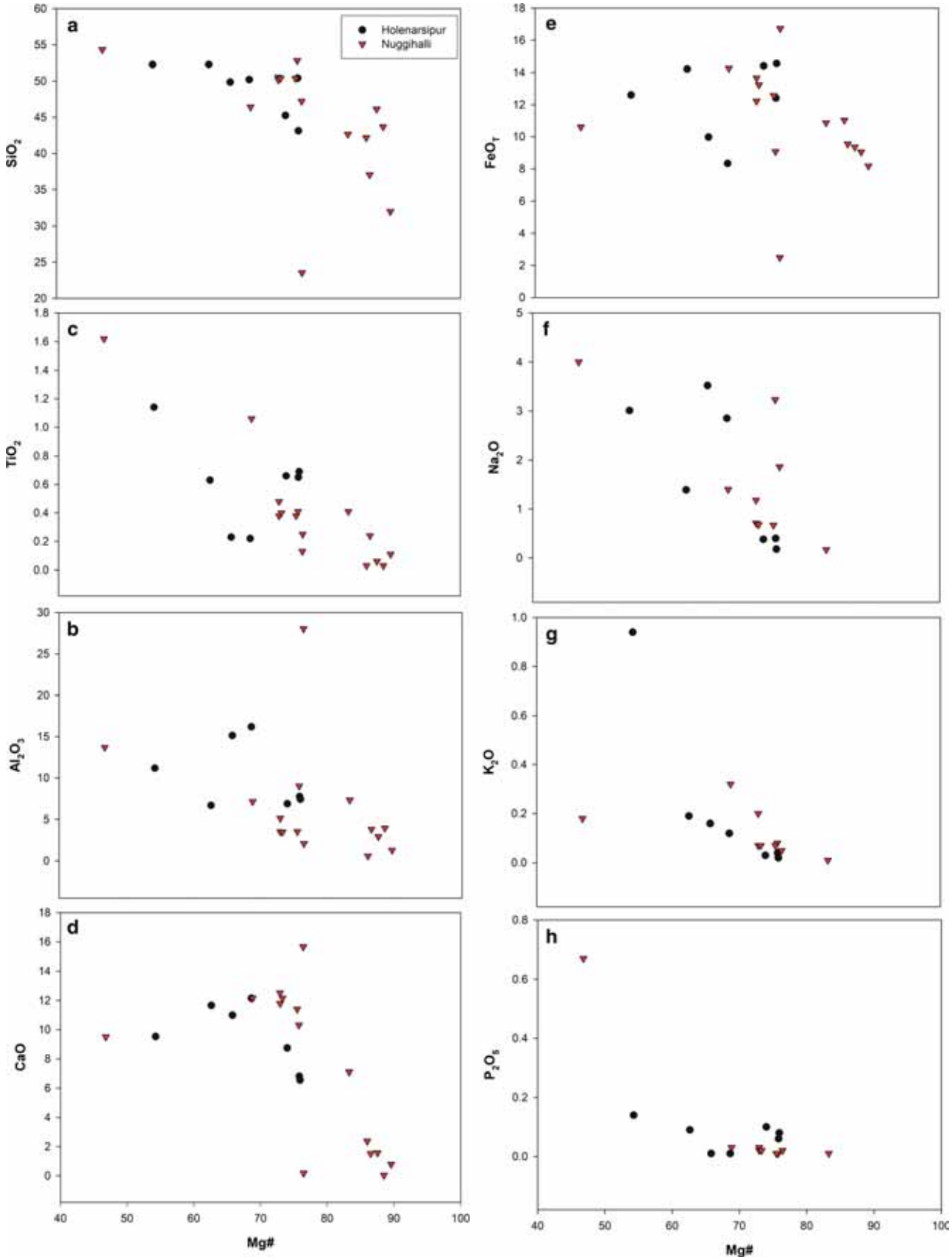

Figure 4. Major element oxides *vs.* Mg# plots (Harker's plots) for the rocks of HGB and NGB.

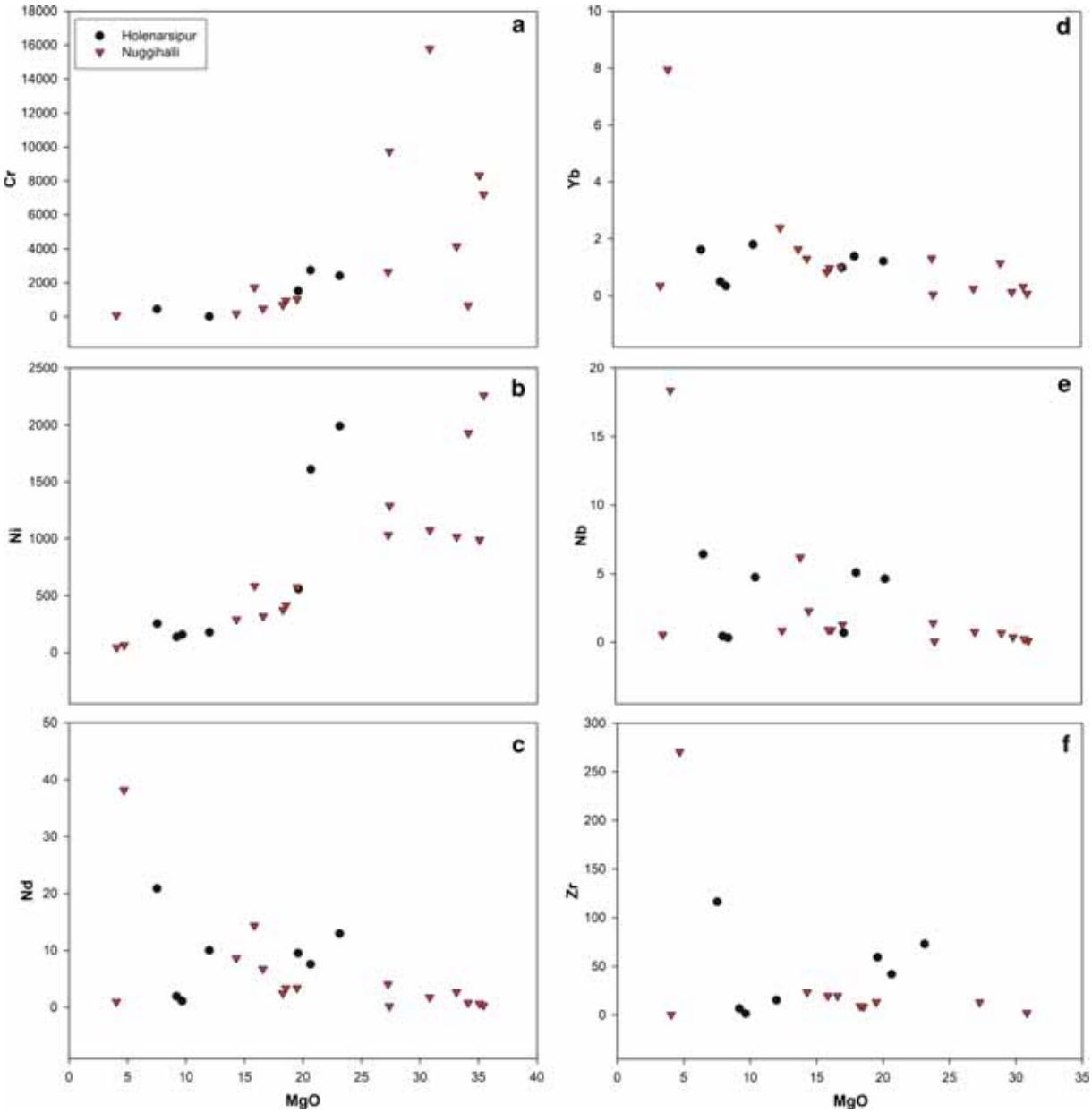

Figure 5. Selected trace elements *vs.* MgO plots for the rocks of HGB and NGB.

from Jamburu, NH-12, when considered along with the ultramafic rock samples from the same mine, NH-10 and NH-11, shows complementary enrichment in Eu with respect to the ultramafic samples, corroborating with the observations made in the major oxides *vs.* MgO plots (figure 4). The amphibole-rich sample, NH-14, composed of hornblende, actinolite and minor quartz, collected from the upper bench of the Jamburu mine, exhibits flat chondrite-normalized REE pattern with pronounced negative Eu anomaly (figure 7c). The mafic rock samples from Tagadur mine (NH-03, NH-17 and NH-18) all have a near flat chondrite normalized REE pattern with negligible LREE enrichment (figure 7c). Their $(La/Yb)_N$, $(La/Sm)_N$ and $(Gd/Yb)_N$ ratios for range from 1.12 to 3.25, 0.63 to 1.48 and 1.33 to 2.30, respectively (table 1).

In the primitive mantle normalized diagram (figure 8) Cs, Rb, Sr and Pb are not included considering their mobility. The HGB samples show a slight enrichment in the incompatible trace elements (figure 8a). The NGB samples (figure 8b and c) show comparable patterns for the mafic and ultramafic rocks with the latter rocks having generally lower abundances for most elements.

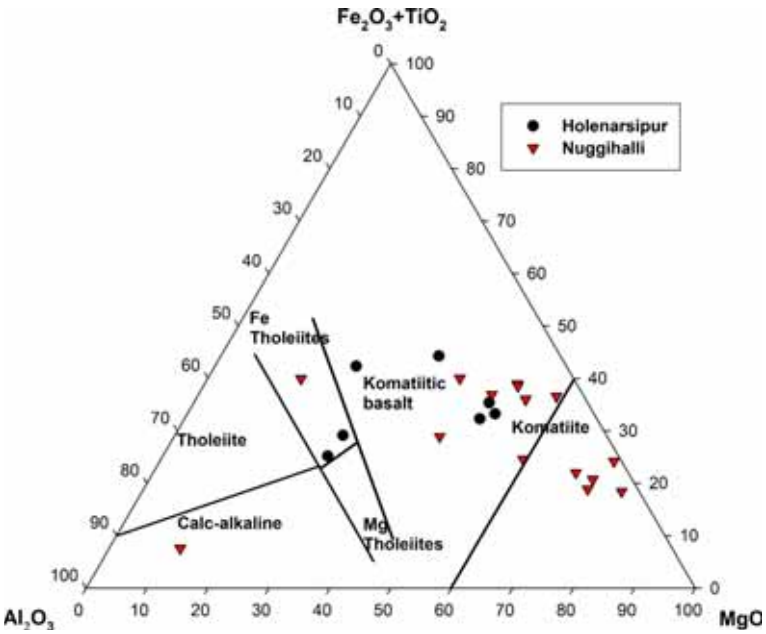

Figure 6. Triangular plot showing the compositional classification of the rocks of the HGB and NGB (after Jensen 1976 and Viljoen and Viljoen 1982).

6. Discussion

6.1 *Element mobility*

The progressive increase in the Ni and Cr concentration with increase in MgO (figure 5) indicates olivine fractionation was controlling the distribution of these trace elements. Fractionation of orthopyroxene and clinopyroxene, as well as, primary hornblende from a parental basaltic magma can also affect the distribution of Cr owing to its greater partitioning coefficient in these minerals in basaltic and basaltic–andesitic liquids compared to olivine (Rollinson 1993). The parallel chondrite-normalized REE patterns for the mafic and ultramafic rocks from NGB (figure 7b and c) are indicative of the closed petrogenetic relations between them. When the mafic and ultramafic rocks are considered together, they show a narrow range in La/Sm (0.6–3.5), Sm/Yb (0.5–2.0) and La/Yb (0.6–4.8) ratios suggesting differentiation processes only to have caused the observed REE concentrations in them. Similar parallelism can be observed in the chondrite-normalized REE patterns (figure 7a) of the mafic and ultramafic rocks of HGB (HN-10, 24, 28 and 33), though these rocks show a greater enrichment in the LREE. A positive trend (with a gentle slope) observed for samples from HGB and those from individual sampling locations (Tagadur, Jamburu and Bhaktarahalli) of NGB in the La/Sm *vs.* La plot (figure 9a) is also suggestive of crystal-liquid fractionation processes to have influenced the observed incompatible element ratios.

In the Zr/Zr* and Hf/Hf* *vs.* CaO/Al_2O_3 plots (after Lahaye *et al.* 1995), the latter ratios remain more or less constant with no significant trend for the ultramafic rocks of the studied areas (figure 9b and c). This also indicates magmatic processes were responsible for the distribution of trace elements between the different rock units. The near parallel trace element patterns (figures 7 and 8) for the mafic as well as ultramafic rocks suggest that mobility due to hydrothermal alteration and/or metamorphism of the elements considered has been minor. The sepentinization of the primary rocks due to the interaction of circulating fluids could cause mobility to several geochemical elements such as HFSE. Nevertheless, the nature of the fluids is an important factor to be considered while discussing mobility of the relatively immobile REE and other HFSE. Involvement of carbonate ion has been shown to be essential for the mobility of the HFSE, particularly REE (Fryer *et al.* 1979; Hynes 1980; Ludden *et al.* 1984; McCulloch and Black 1984; Windrim *et al.* 1984; Murphy and Hynes 1986; King and Kerrich 1987; Rubin *et al.* 1988, 1993; Wood 1990; Bau 1991; Tourpin *et al.* 1991; Gruau *et al.* 1992; Bau and Knittel 1993; Lahaye *et al.* 1995; Lahaye and Arndt 1996; Ordóñez-Calderón *et al.* 2008). Due to near absence of carbonate minerals, no significant involvement

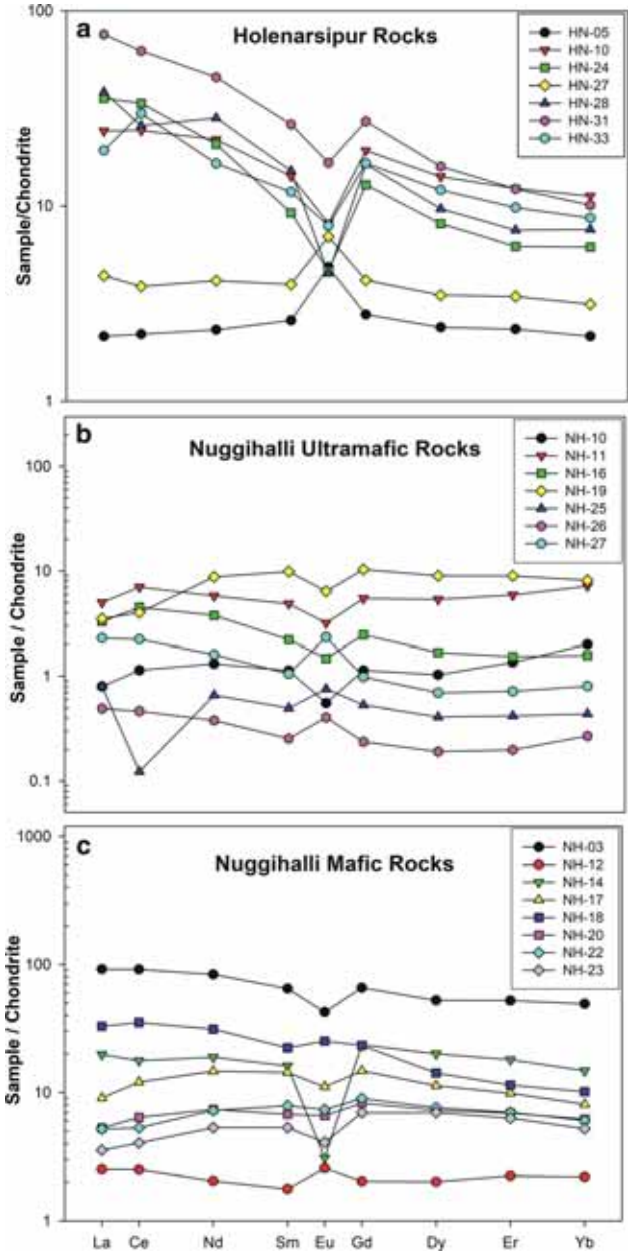

Figure 7. Chondrite normalized REE plots for the ultramafic and mafic rocks of the HGB and NGB.

of CO_2-enriched fluids is inferred in these rocks, unlike in the rocks of the Sargur type area south of Mysore, where network patterns of magnesite veins are abundant. Therefore, the rocks of HGB and NGB can be presumed to have been resistant to mobility of HFSE during the later alteration and metamorphism.

The primitive mantle normalized multielement diagrams (figure 8) show significant Nb and Ti anomaly in most of the samples of the greenstone belts studied in the present work. While the presence of layers of vanadiferous titaniferous magnetite may be the concentrator of Ti imparting a Ti negative anomaly to the ultramafic and mafic rocks, fractionation of minerals such as Mg-perovskite (Kato *et al.* 1996; Taura *et al.* 2001; Corgne *et al.* 2005; Robin-Popieul *et al.* 2012), known to concentrate Nb, Ti, Zr and Hf, during the early stages of magmatic history could also have developed the negative anomalies in these elements. Alternatively, contamination from an older crust, closer to the subduction front, could also have given negative anomalies to the ensuing melts, particularly for the rocks of the HGB where significant LREE enrichment is also observed in most of the samples (figure 7a).

6.2 *Lithological variations and crustal thickness*

The mafic and ultramafic rocks of HGB and NGB are considered to be related suites of rocks in which the compositional variations observed are a consequence of crystal–liquid fractionation processes in individual greenstone belts. The presence of layered igneous structure (figure 2e), particularly well preserved in the Nuggihalli greenstone belt, can be corroborated with the correlations observed in the Harker plots (figures 4 and 5). The ultramafic–mafic rock formations of these two belts are noticeably different in their lithological association. The HGB is less dominated by ultramafic rocks such as serpentinized peridotites and chromitites in comparison to the NGB. While the near complete ultramafic layered sequence is preserved in the chromite mines of NGB, only sporadic distribution of peridotites and the upward sequence differentiates such as anorthosite and gabbro are exposed in the HGB. Geophysical studies (Gupta *et al.* 2003; Rai *et al.* 2013) have indicated increase in the crustal thicknesses westward from the EDC to the WDC in the regions of flatter topography. The location of NGB in the MOHO depth map (figure 9a of Rai *et al.* 2013) is closer to the 44 km depth contour while the location of HGB, situated at around 40 km SE of NGB, is near the 48 km depth contour. The 4 km difference in the crustal thickness in these two localities, which are essentially at the same topographic elevation, could explain the preservation of shallower lithologies in HGB. The exposures of deeper lithologies are therefore preserved in the NGB as compared to HGB. Similar variations in crustal thickness are also noticed in the WDC from north to south (Drury *et al.* 1984; Rai *et al.* 2013).

Table 1. *Major (wt%) and trace element (ppm) concentrations of ultramafic and mafic rock samples of Holenarsipur and Nuggihalli greenstone belts, western Dharwar craton.*

	Ultramafic rocks										BCR-2	
	HN-24	HN-28	HN-33	NH-10	NH-11	NH-16	NH-19	NH-25	NH-26	NH-27	Measured	Reported
SiO_2	50.42	43.14	45.26	43.68	46.13	37.05	42.66	32.01	23.54	42.18	53.0	54.10
TiO_2	0.65	0.69	0.66	0.03	0.06	0.24	0.41	0.11	0.25	0.03	2.3	2.26
Al_2O_3	7.76	7.42	6.88	3.96	2.94	3.82	7.33	1.29	2.09	0.58	13.6	13.50
MnO	0.20	0.17	0.20	0.08	0.16	0.30	0.15	0.25	0.65	0.15	ND	0.20
Fe_2O_3	12.41	14.56	14.41	9.05	9.36	9.55	10.87	8.18	16.73	11.03	13.6	13.80
CaO	6.82	6.56	8.74	0.03	1.57	1.52	7.11	0.79	0.18	2.37	6.9	7.12
MgO	19.59	23.13	20.65	35.08	33.12	30.83	27.27	35.42	27.38	34.11	3.7	3.59
Na_2O	0.40	0.18	0.38	bdl	bdl	bdl	0.17	bdl	bdl	bdl	3.2	3.16
K_2O	0.04	0.02	0.03	bdl	bdl	bdl	0.01	bdl	bdl	bdl	1.8	1.79
P_2O_5	0.06	0.08	0.10	bdl	bdl	bdl	0.01	bdl	bdl	bdl	0.4	0.35
LOI	1.32	3.50	2.21	6.00	5.91	4.99	3.57	13.60	6.91	9.09		
Total	99.67	99.45	99.52	97.91	99.25	88.30	99.56	91.65	77.73	99.54		
Mg#	75.8	75.9	74.0	88.5	87.5	86.5	83.3	89.6	76.5	86.0		
Cr	1522	2412	2738	13274*	4310*	78891*	2640	54943*	149846*	958	17.0	18.0
Ni	561	1990	1610	988	1016	1075	1031	2257	1288	1929	27.0	18.0
Sc	23.3	13.6	15.1	9.0	18.3	9.1	26.5	7.3	3.9	8.3	42.0	33.0
V	174	138	157	66.9	54.6	38.6	178	24.4	38.2	22.8	505	416
Cs	0.08	0.03	0.09	0.11	0.07	0.22	0.28	0.14	0.29	0.16	1.20	1.10
Rb	0.69	0.04	0.40	0.03	0.06	0.02	0.35	0.07	0.08	bdl	55.0	48.0
Sr	10.0	8.40	9.74	2.45	2.19	3.71	5.82	22.5	6.95	75.5	374	346
Pb	1.10	1.37	0.64	0.35	0.18	0.48	0.34	1.01	1.42	1.27	10.0	11.0
Th	2.43	1.06	1.01	0.11	0.15	0.41	0.08	0.07	0.06	0.06	6.20	5.70
U	0.57	0.16	0.13	0.04	0.03	0.05	0.04	0.03	0.03	0.07	1.70	1.69
Nb	0.68	4.63	5.08	0.22	0.66	0.74	1.39	0.09	0.04	0.36	16.0	12.6
Ta	0.08	0.28	0.37	0.02	0.04	0.07	0.09	0.02	0.01	0.02	0.84	0.74
Zr	59.4	73.0	42.1	bdl	bdl	2.04	13.0	bdl	bdl	bdl	221	184
Hf	1.66	1.83	1.17	0.06	0.11	0.14	0.41	0.08	0.06	0.07	4.90	4.90
Ti	3895	4135	3955	180	360	1438	2457	659	1498	180	13784	13500
Y	14.3	15.3	19.1	1.82	8.01	3.12	12.6	0.87	0.55	1.32	44.0	37.0
La	8.47	9.12	4.57	0.19	1.19	0.78	0.83	0.19	0.12	0.54	28.0	24.9
Ce	20.6	15.8	18.3	0.70	4.31	2.76	2.46	0.08	0.29	1.37	59.0	52.9
Nd	9.49	12.9	7.54	0.60	2.64	1.73	4.02	0.30	0.17	0.73	30.0	28.7
Sm	1.36	2.24	1.75	0.17	0.72	0.33	1.46	0.07	0.04	0.16	7.0	6.58
Eu	0.26	0.25	0.45	0.03	0.18	0.08	0.36	0.04	0.02	0.13	2.0	1.96
Gd	2.55	3.26	3.29	0.23	1.09	0.49	2.06	0.11	0.05	0.20	7.0	6.75
Dy	1.99	2.38	2.97	0.25	1.32	0.41	2.22	0.10	0.05	0.17	7.4	6.41

Table 1. *(Continued.)*

	Ultramafic rocks										BCR-2	
	HN-24	HN-28	HN-33	NH-10	NH-11	NH-16	NH-19	NH-25	NH-26	NH-27	Measured	Reported
Er	0.99	1.20	1.57	0.22	0.94	0.25	1.44	0.07	0.03	0.11	3.9	3.66
Yb	0.99	1.22	1.40	0.32	1.15	0.25	1.31	0.07	0.04	0.13	3.5	3.38
Lu	0.02	0.06	0.11	0.06	0.16	0.03	0.18	0.01	0.00	0.02	0.5	0.503
ΣREE	46.8	48.5	41.9	2.77	13.7	7.11	16.3	1.04	0.81	3.56		
Nb/Yb	0.69	3.80	3.64	0.70	0.57	2.93	1.06	1.25	1.01	2.79		
Th/Yb	2.45	0.87	0.72	0.34	0.13	1.63	0.06	0.93	1.42	0.48		
Al_2O_3/TiO_2	11.9	10.8	10.4	132	49.0	15.9	17.9	11.7	8.36	19.3		
CaO/Al_2O_3	0.88	0.88	1.27	0.01	0.53	0.40	0.97	0.61	0.09	4.09		
$(La/Yb)_N$	5.79	5.08	2.22	0.40	0.70	2.09	0.43	1.82	1.83	2.86		
$(La/Sm)_N$	3.88	2.54	1.63	0.71	1.03	1.48	0.36	1.61	1.94	2.18		
$(Gd/Yb)_N$	2.08	2.16	1.91	0.57	0.76	1.57	1.27	1.21	0.88	1.22		
$(Sm/Nd)_N$	0.44	0.54	0.71	0.86	0.84	0.59	1.12	0.75	0.67	0.66		
Eu/Eu*	0.43	0.29	0.57	0.49	0.62	0.63	0.63	1.47	1.65	2.30		
Nb/Nb*	0.05	0.51	0.80	0.52	0.54	0.44	1.80	0.26	0.17	0.68		
Zr/Zr*	1.15	0.94	0.80	–	–	0.19	0.37	–	–	–		
Hf/Hf*	1.16	0.85	0.81	0.45	0.19	0.47	0.43	1.33	1.77	0.56		

	Mafic rocks											
	HN-05	HN-10	HN-27	HN-31	NH-03	NH-12	NH-14	NH-17	NH-18	NH-20	NH-22	NH-23
SiO_2	49.87	52.30	50.22	52.28	54.34	47.23	52.81	50.54	46.43	50.38	50.20	50.40
TiO_2	0.23	0.63	0.22	1.14	1.62	0.13	0.41	0.48	1.06	0.38	0.38	0.40
Al_2O_3	15.14	6.68	16.20	11.19	13.71	28.03	9.02	5.14	7.14	3.54	3.52	3.49
MnO	0.13	0.25	0.14	0.18	0.12	0.02	0.15	0.22	0.21	0.18	0.20	0.23
Fe_2O_3	9.98	14.21	8.34	12.60	10.61	2.49	9.08	12.22	14.26	12.57	13.66	13.23
CaO	10.99	11.66	12.15	9.53	9.50	15.67	10.31	12.52	12.16	11.40	11.79	12.16
MgO	9.67	11.99	9.19	7.53	4.70	4.06	14.29	16.58	15.85	19.49	18.54	18.28
Na_2O	3.52	1.39	2.85	3.01	4.00	1.86	3.23	1.18	1.40	0.67	0.71	0.68
K_2O	0.16	0.19	0.12	0.94	0.18	0.05	0.08	0.20	0.32	0.07	0.07	0.07
P_2O_5	0.01	0.09	0.01	0.14	0.67	0.02	0.01	0.02	0.03	0.01	0.03	0.02
LOI	0.21	0.50	0.46	1.23	0.50	0.40	0.47	0.78	0.80	1.13	0.72	0.90
Total	99.91	99.89	99.90	99.77	99.95	99.96	99.86	99.88	99.66	99.82	99.82	99.86
Mg#	65.8	62.6	68.6	54.3	46.8	76.4	75.8	72.9	68.8	75.5	72.9	73.3
Cr	bdl	9.26	bdl	438	bdl	82.9	176	469	1719	1018	934	688
Ni	158	178	137	255	64.1	44.0	290	319	586	573	418	375
Sc	18.4	29.6	19.5	30.9	29.4	8.43	11.7	42.3	18.1	41.6	9.42	55.5
V	131	209	104	252	330	87	152	169	218	154	158	195
Cs	0.15	0.07	0.08	0.66	0.03	0.004	0.004	0.04	0.26	0.72	0.30	0.18

Table 1. *(Continued.)*

	Mafic rocks											
	HN-05	HN-10	HN-27	HN-31	NH-03	NH-12	NH-14	NH-17	NH-18	NH-20	NH-22	NH-23
Rb	1.78	2.83	1.51	26.5	2.61	0.06	0.14	2.23	1.55	0.73	0.54	0.18
Sr	324	106	261	301	117	56.7	84.9	62.1	32.5	11.4	10.8	8.22
Pb	0.84	2.49	1.16	5.57	1.56	0.66	0.42	0.85	0.73	0.98	1.00	1.71
Th	0.07	0.95	0.17	2.71	3.55	0.11	0.15	0.41	0.73	0.18	0.11	0.16
U	0.02	0.27	0.05	0.59	0.84	0.05	0.12	0.07	0.16	0.07	0.07	0.05
Nb	0.33	4.74	0.44	6.41	18.4	0.54	0.84	2.27	6.17	1.28	0.88	0.89
Ta	0.04	0.43	0.14	0.44	1.32	0.06	0.01	0.19	0.44	0.09	0.06	0.07
Zr	1.37	15.2	6.57	116	271	0.36	23.3	19.5	19.6	13.2	8.47	8.98
Hf	0.17	0.66	0.34	2.87	6.43	0.16	1.11	0.79	0.92	0.54	0.36	0.47
Ti	1378	3776	1318	6832	9709	779	2457	2877	6353	2277	2277	2397
Y	3.78	20.5	5.35	21.3	79.6	2.89	23.7	15.0	18.3	9.98	8.42	10.1
La	0.51	5.75	1.04	17.95	21.7	0.60	4.71	2.15	7.84	1.26	1.23	0.84
Ce	1.35	14.9	2.38	38.1	56.1	1.54	10.9	7.42	21.6	3.93	3.26	2.48
Nd	1.06	10.0	1.90	20.9	38.2	0.93	8.64	6.72	14.3	3.38	3.33	2.44
Sm	0.38	2.10	0.59	3.89	9.60	0.26	2.40	2.13	3.31	1.00	1.17	0.79
Eu	0.27	0.46	0.39	0.94	2.39	0.15	0.17	0.62	1.43	0.37	0.42	0.23
Gd	0.55	3.83	0.83	5.40	13.1	0.40	4.72	2.95	4.65	1.65	1.79	1.39
Dy	0.59	3.47	0.86	3.92	12.9	0.50	4.95	2.79	3.51	1.80	1.88	1.72
Er	0.37	1.97	0.55	1.96	8.35	0.36	2.90	1.58	1.84	1.11	1.12	1.01
Yb	0.35	1.81	0.51	1.62	7.94	0.35	2.39	1.31	1.64	1.00	0.98	0.84
Lu	0.05	0.15	0.07	0.11	0.99	0.05	0.20	0.17	0.15	0.13	0.14	0.10
ΣREE	5.48	44.5	9.11	94.8	171	5.14	42.0	27.9	60.3	15.6	15.3	11.8
Nb/Yb	0.94	2.62	0.87	3.95	2.31	1.52	0.35	1.74	3.77	1.28	0.91	1.05
Th/Yb	0.20	0.53	0.33	1.67	0.45	0.32	0.06	0.31	0.44	0.18	0.12	0.19
Al_2O_3/TiO_2	65.8	10.6	73.6	9.82	8.46	216	22.0	10.7	6.74	9.32	9.26	8.73
CaO/Al_2O_3	0.73	1.75	0.75	0.85	0.69	0.56	1.14	2.44	1.70	3.22	3.35	3.48
$(La/Yb)_N$	1.00	2.16	1.40	7.51	1.86	1.15	1.34	1.12	3.25	0.85	0.86	0.68
$(La/Sm)_N$	0.83	1.71	1.11	2.88	1.41	1.43	1.23	0.63	1.48	0.78	0.66	0.67
$(Gd/Yb)_N$	1.29	1.71	1.33	2.69	1.33	0.93	1.60	1.83	2.30	1.34	1.49	1.33
$(Sm/Nd)_N$	1.12	0.65	0.96	0.57	0.78	0.87	0.86	0.98	0.71	0.92	1.09	1.00
Eu/Eu*	1.81	0.49	1.71	0.62	0.65	1.36	0.16	0.76	1.11	0.88	0.87	0.67
Nb/Nb*	0.59	0.69	0.36	0.31	0.71	0.69	0.34	0.82	0.88	0.93	0.80	0.83
Zr/Zr*	0.15	0.23	0.43	0.89	0.98	0.05	0.35	0.36	0.20	0.37	0.49	0.30
Hf/Hf*	0.66	0.36	0.81	0.80	0.84	0.80	0.61	0.53	0.34	0.74	0.46	0.84

Bdl below the limit of detection, *ND* not determined.

*Cr for samples NH-10, NH-16, NH-25 and NH-26 were determined by X-Ray Fluorescence Spectrometry.

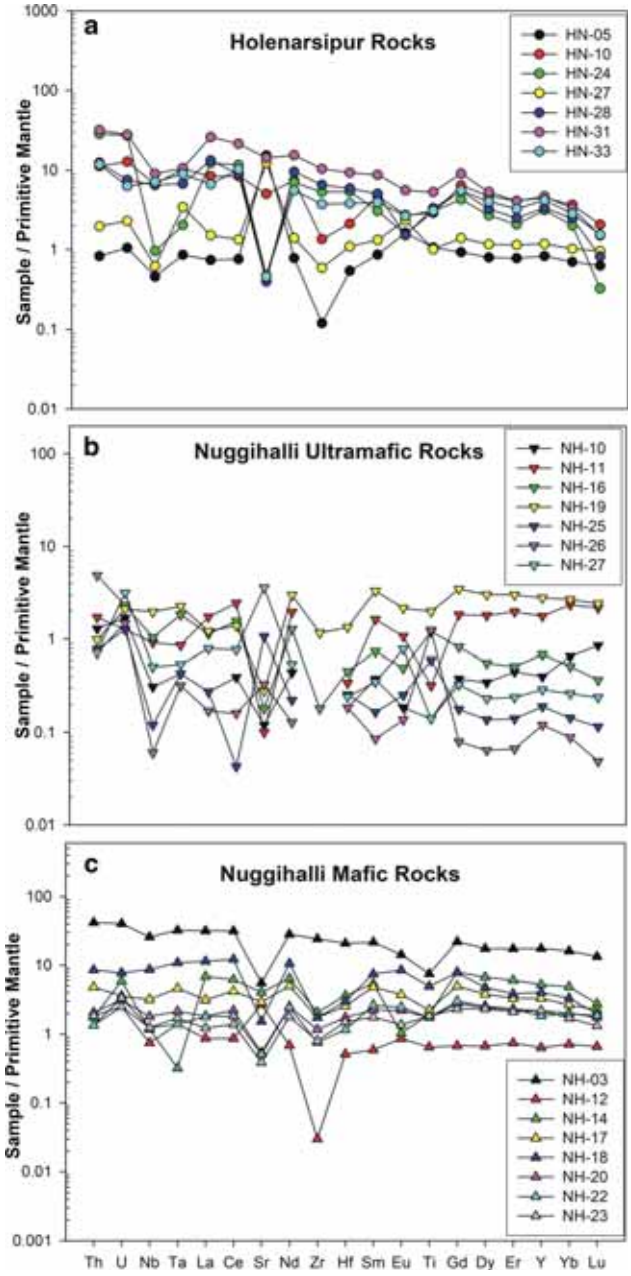

Figure 8. Primitive mantle normalized trace element plots for the ultramafic and mafic rocks of the HGB and NGB.

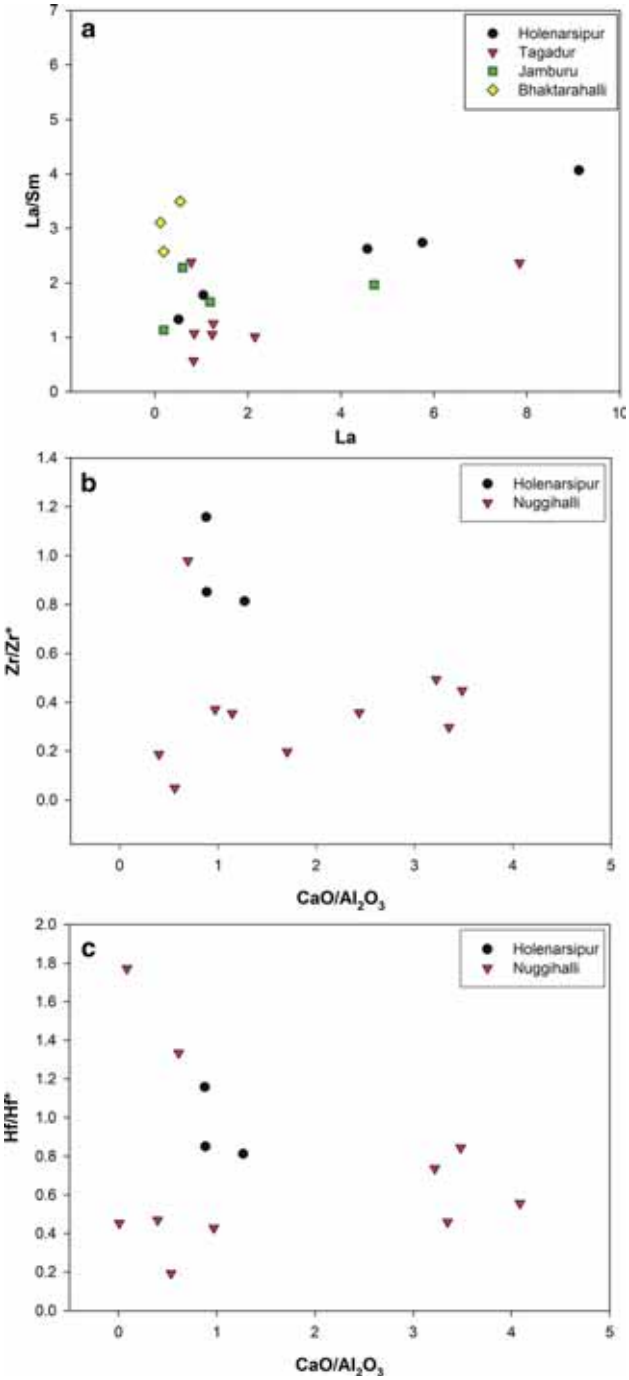

Figure 9. (**a**) La/Sm *vs.* La plot for mafic–ultramafic rock samples from Holenarsipur and Nuggihalli (Tagadur, Jamburu and Bhaktarahalli); **(b)** Zr/Zr* *vs.* (CaO/Al_2O_3) plot for the ultramafic rock samples from HGB and NGB (ratios are given in table 1); **(c)** Hf/Hf* *vs.* (CaO/Al_2O_3) plot for the ultramafic rock samples from HGB and NGB (ratios are given in table 1) (Plots b and c are after Lahaye *et al.* 1995).

Therefore, though the HGB and NGB may represent preserved ultramafic–mafic crust of Sargur affinity, the noticeable difference in the lithological association may be due to the different crustal levels that are exposed in the present day. This may imply measurable time variations in the emplacement of the precursor rocks of these greenstone belts. Also, the distribution of trace elements, which was probably controlled by the magmatic differentiation processes, may be significantly different in the rocks of these belts. In the further discussion, 5 the rocks of the NGB are considered to represent crustal levels relatively deeper than those for the rocks of the HGB, though no significant differences in their grades of metamorphism is noticed.

6.3 *Significance of Al-depletion*

Komatiites from many of the Archean greenstone belts are usually distinguished based on the degree of Al-depletion or Al-enrichment and are therefore broadly classified into Al-depleted Barberton-type, Al-undepleted Munro-type and Al-enriched Gorgona-type Cretaceous komatiites (Arndt 2008 and references therein). It has also been observed that the Al-depletion is a characteristic of older komatiites such as in Barberton while progressively younger komatiites are represented by Al-undepleted and Al-enriched types. However, Chavagnac (2004) has shown that in the Komati formation of Barberton greenstone belt, both Al-depleted and Al-undepleted types occur. Ohtani *et al.* (1989) attributes the occurrence of different Al-types of komatiites to mantle heterogeneity or to chemical layering of the mantle. Jayananda *et al.* (2008) also report the occurrence of both Al-depleted and Al-undepleted komatiites from the Sargur Group of rocks of Dharwar craton. As stated before, the greenstone belts of Sargur Group that expose komatiites are mostly dominated by intrusive and layered ultramafic rocks with only a thin veneer of komatiites possibly overlying as a supracrustal sequence. In the NGB during the present study it was found that true komatiites or komatiitic basalts are insignificant except for earlier reports of their occurrence (Jafri *et al.* 1997). The outcrops and the exposures in the mine cuttings are dominantly peridotitic and have a komatiitic to komatiitic basaltic composition. Here we employ the Al-depletion criterion to the ultramafic–mafic rocks of the layered igneous complex of NGB and HGB and attempt to evaluate its significance in understanding processes that impart Al-depleted and Al-undepleted signatures to these rocks.

The ultramafic–mafic rocks of the HGB and NGB, considered as compositional equivalents of komatiites and komatiitic basalts, are a combination of Al-depleted and Al-undepleted rocks based on the Al_2O_3/TiO_2 and CaO/Al_2O_3 *vs.* $(Gd/Yb)_N$ plots (figure 10). All of the ultramafic rock samples from HGB are Al-depleted. The Al-depleted signature is indicative of the presence of garnet in the residue during the generation of the melt. Alternatively, garnet was fractionally crystallized from ultramafic magmas (Green 1975; Ohtani 1984; Arndt 2008). If the rocks of the HGB are considered to have formed from the residual liquid left after the fractionation of an early assemblage containing garnet, they can show an Al-depleted

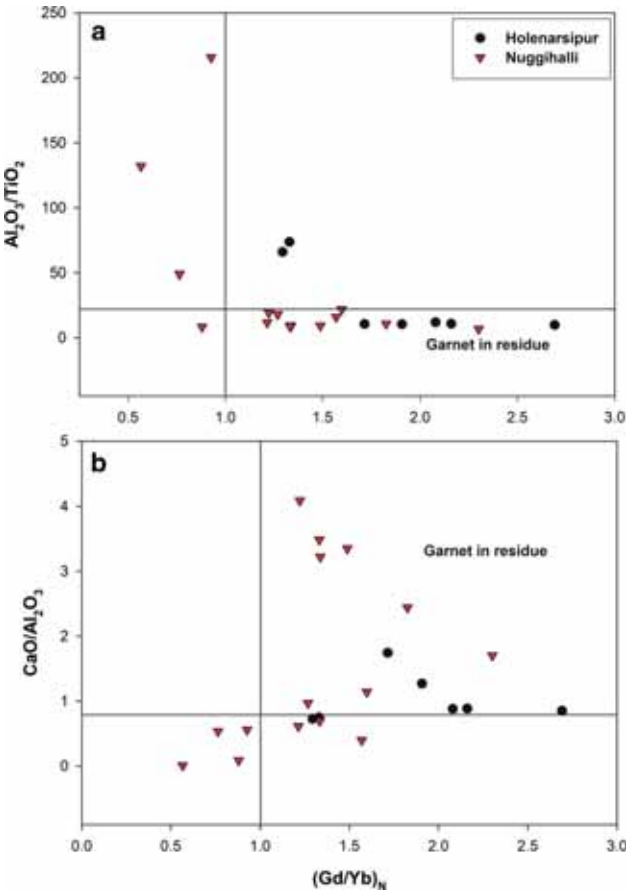

Figure 10. Al_2O_3/TiO_2 and CaO/Al_2O_3 *vs.* $(Gd/Yb)_N$ plots for the ultramafic and mafic rocks of HGB and NGB.

signature. The ultramafic rocks (HN-24, HN-28 and HN-33) and mafic rocks (HN-10 and HN-31) of the HGB have higher $(Gd/Yb)_N$ ratios > 1. This could indicate that garnet was not present in the melt that generated the ultramafic–mafic rocks of the HGB, implying a deeper origin for the parental melts. However, if fractional crystallization was the dominant process that imparted geochemical characteristics, then exclusion of garnet in the fractionated phases can also give rise to the observed Al-depleted signature, considering the rocks to be cumulates. The samples HN-05 and HN-27, however, are the plagioclase-rich later intrusive rocks that have a much elevated Al_2O_3/TiO_2 ratios (65.83 and 73.64, respectively). Their $(Gd/Yb)_N$ ratios are >1 precluding role of garnet in their alumina enrichment.

The LREE enriched chondrite normalized REE patterns (figure 7a) for the ultramafic as well as mafic rocks of the HGB may be due to the fractionation of relatively MREE and HREE enriched mineral phases such as amphiboles and pyroxenes during different stages of differentiation. Cumulus,

intercumulus and postcumulus occurrence of hornblende in ultramafic intrusions have been reported from Archean Stillwater and Fiskenæsset Complexes (Page and Zientek 1987; Polat *et al.* 2012) and from Phanerozoic Lilloise intrusion (Brown *et al.* 1982). The LREE enrichment could also be due to contamination from older crust. Such an enriched pattern is not observed in the rocks of the Nuggihalli greenstone belt which show flat REE patterns with slight LREE enrichment in some samples.

In the rocks of the Nuggihalli greenstone belt, which show clear development of layering indicating fractional crystallization from the primary melt, garnet may have occurred as a fractionating phase in the Al-undepleted rocks resulting in Al-depleted signature in later liquids that crystallized to produce more evolved rocks of the belt. For the generation of ultramafic magmas by melting, it has been suggested that during high P melting, garnet is largely left in the residue and the participation of garnet in the melting can only be initiated at lower P (Green 1975; Ohtani *et al.* 1989; Zhang and Herzberg 1994; Robin-Popieul *et al.* 2012). The parent melt, however, might have had variable presence of garnet both in the residue and as a melting phase. This suggests the generation of melts at variable depths and their migration due to density contrast with the unmelted refractory residue and subsequent melting of the residue itself. The initial melts then acquire Al-depletion while the refractory residue gives rise to Al-undepleted/enriched signature for the ensuing melts.

Alternatively, considering the different units of the layered complex were developed during intrusion of the parental melt, the elemental abundances observed in them could be a consequence of fractional crystallization processes. In such a case, the initial crystallization of a spinifex-textured komatiitic ultramafic rock from a high-Mg mafic magma, at the interface with the water saturated ocean floor, could have resulted in Al-depletion. This scenario is possible as aluminium-rich phases could have remained in equilibrium with the residual melt at low pressure conditions. The subsequent fractional crystallization of olivine, pyroxene and plagioclase from the intruding magma could have produced Al-undepleted and Al-depleted rocks as aluminium-rich phases also get fractionated due to the final solidification of the magma.

Role of primary hornblende in the generation of Al-undepleted rocks also needs to be considered. Whether the dominant process was melting or fractional crystallization, it requires an upwelling mantle as in a rising plume or in a mid-oceanic ridge for imparting the observed geochemical characteristics. Maya *et al.* (2016) have suggested two episodes of melting for the sources of Banasandra komatiites that occur further east of NGB. Robin-Popieul *et al.* (2012) have suggested that the presence of Al-depleted to Al-enriched komatiites in the Barberton greenstone belt to be a consequence of different depths of their genesis, with the Al-depleted komatiites generated at depths >9 GPa and shallower depths for the genesis of Al-undepleted and Al-enriched komatiites. Robin-Popieul *et al.* (2012) have also shown that high temperature favours the generation of Al-depleted komatiites. However, at very high temperatures Al-depleted komatiites are not produced as garnet reaches exhaustion before the migration of the melt is effected due to density contrast. Therefore, at very high temperatures, Al-undepleted komatiite generation is favoured (Robin-Popieul *et al.* 2012). Going by the partial melting model for the NGB rocks of komatiitic composition, the generation of the parent melts should have been at sufficiently high temperatures and pressures to produce predominantly Al-depleted rocks while the later melts became progressively less depleted eventually giving rise to Al-undepleted basalts.

However, in the exposed layered complex in the mine sections at Jamburu and Tagadur areas of NGB, chlorite schists and ultramafic rocks rich in hornblende that are presumed to be primary cumulates are present along with gabbro and anorthosite. Hornblendite layers also are present and have been reported from other greenstone belts of Sargur Group (Swami Nath and Ramakrishnan 1981; Jayananda *et al.* 2008). As an alternative to deep seated melting processes, the Al–Ti and Gd–Yb signatures observed in the rocks of the belt could also be attributed to the fractionation of primary hornblende and plagioclase from a high-Mg basaltic melt. The $(Gd/Yb)_N$ ratio slightly greater than one in most samples does not indicate the role of garnet only in the observed ratio. The compositional diversity seen in the rocks of the NGB therefore can be due to impendent fractional crystallization processes during the formation of the layers at shallower crustal levels. The implication of this inference is, when a hypothetical bulk composition of the magma column is considered, the primary melt need not be ultramafic and the

melting of the mantle could have been at much lower pressures as encountered at the upwelling mantle at a mid-ocean ridge. Also, the upper mantle was sufficiently hydrous during the Archean and was a contributor in the development of layered igneous complexes (Polat *et al.* 2012). The trace element signatures in the Th/Yb *vs.* Nb/Yb diagram after Pearce (2008) (figure 11) also indicate absence of unequivocal OIB signatures in the basalts. Figure 11 shows two samples from HGB and NGB plotting in the Mantle Array in the MORB field while the rest of the samples plot slightly away from the array with a trend towards the volcanic arc array. The deviation of the sample points from the array could be attributed to interaction with subduction related material or due to contamination by a pre-existing continental crust. The presence of an older crust has been reported from Gorur area near Holenarsipur (Beckinsale *et al.* 1980; Bhaskar Rao *et al.* 1991; Meen *et al.* 1992; Peucat *et al.* 1993; Jayananda *et al.* 2015) implying the probability of crustal contamination, as the mafic–ultramafic magmas are known to underplate older crust and assimilate crustal materials by thermal erosion (Huppert *et al.* 1984; Arndt and Jenner 1986; Williams *et al.* 1998, 2002; Arndt 2008).

6.4 *Fractional crystallization modelling*

To test the above hypothesis, fractional crystallization of an assemblage consisting of 50% olivine, 40% orthopyroxene, 3% clinopyroxene and 7% plagioclase was modelled based on the normative mineralogy of sample NH-10, a peridotitic komatiite from the lower part of Jamburu mine, assuming it to fractionate from a hypothetical primary melt akin to NH-14, a high-Mg basalt (table 1) collected from the upper benches of the mine (figure 12). It can be seen from the figure that fractional crystallization of the assemblage considered enriches the residual melt in their overall REE content without significantly affecting the chondrite normalized pattern. But the instantaneous solid comprising the assemblage produced by even about 10% fractional crystallization shows a relative enrichment in the HREE (figure 12). The hypothetical initial composition represented by the sample NH-14 has a $(Gd/Yb)_N > 1$, while the product of fractional crystallization results in a $(Gd/Yb)_N < 1$ (figure 12). It is therefore suggested that the observed Al-depleted and Al-undepleted signatures in the NGB rocks are a consequence of fractional crystallization in the magma chamber. The similarities in the chondrite normalized REE patterns for the ultramafic and mafic rocks, with relative enrichment in several rocks of the latter, are better explained by this model. The $(Gd/Yb)_N$ ratio for NH-10 is 0.57 and the observed $(La/Sm)_N$ ratio (figure 12) could be due to appreciable contamination by older crust which did not significantly affect the $(Gd/Yb)_N$ ratio.

6.5 *Implications for mantle heterogeneity and tectonic setting*

The tectonic setting for the emplacement of komatiitic lavas exhibiting spinifex texture and the associated near surface intrusive peridotites during

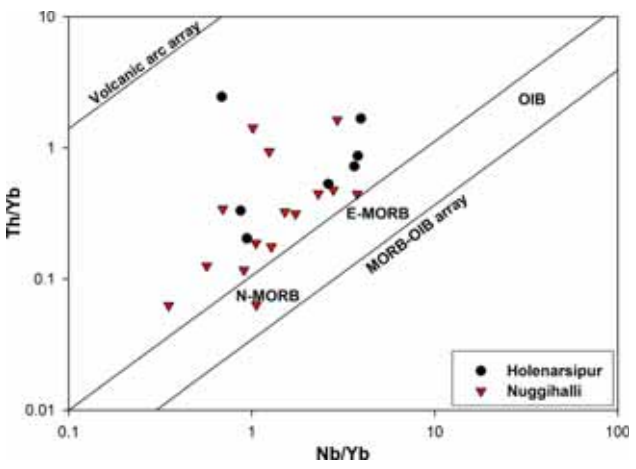

Figure 11. Th/Yb *vs.* Nb/Yb diagram (after Pearce 2008) showing the MORB–OIB array and the distribution of rocks samples from HGB and NGB.

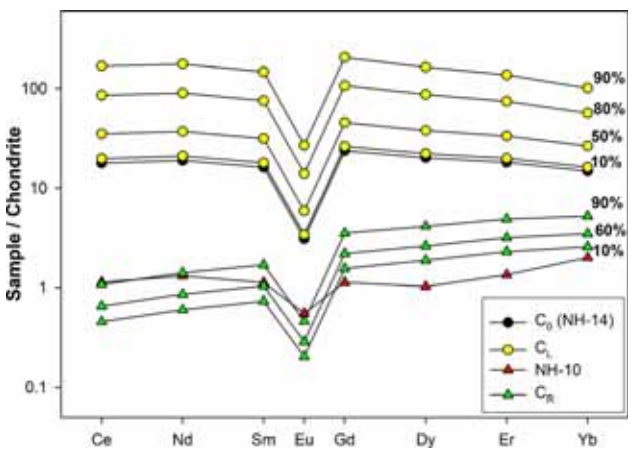

Figure 12. Fractional crystallization modeling starting with a hypothetical sample for different degrees of fractionation showing patterns for the resultant liquids and the fractionating assemblages.

the Archean requires suitable conditions for the mantle to upwell and intersect the Archean geothermal gradient. With the exception of the Cretaceous Gorgona komatiites, the ultramafic extrusive rocks occurring in association with intrusive equivalents are restricted to the Archean. Even within the Archean, the Al-depleted peridotitic komatiites are dominantly abundant in the Mesoarchean while the Al-undepleted and Al-enriched peridotitic komatiites are more common in the Neoarchean greenstone belts indicating evolution in the mantle composition during Archean. The association of Al-depleted and Al-undepleted peridotitic komatiites are encountered at several Mesoarchean greenstone belts (Fan and Kerrich 1997; Arndt 2008; Jayananda *et al.* 2008; Robin-Popieul *et al.* 2012) which implies the possibility of a heterogeneous mantle before crust extraction. Al-depleted komatiites are thought to be produced either by high degree of partial melting at greater depths or by low degree of partial melting at shallower depths (Ohtani 1990). Based on experimental studies, Green (1975) had shown that the association of Archean granite-greenstones with local preservation of thick mafic and ultramafic crust can be explained by a steeper geothermal gradient in a thin lithosphere (about 50 km thick) above the asthenosphere precluding the formation of eclogite and thereby implying unlikelihood of subduction similar to modern processes. Instead, the oceanic crust in the down-going peridotitic lithosphere might get scraped off and folded against or between sialic continental crust(s) (Green 1975). In such a scenario, deep crustal melts will undergo differentiation eventually leading to granitic melt generation and limiting subduction related volcanism. The oceanic crust will then be preserved much similar to the Phanerozoic ophiolites.

Abbott (1996) has argued that ridge-plume interactions can produce thick oceanic crust that will resist subduction and eventually get incorporated into the continental lithosphere. The higher temperatures might keep the upwelling mantle, where a mid ocean ridge interacts with a rising plume, buoyant and accreting into thicker crust preventing its subduction. Such plume-modified ridge subduction model also predicts presence of TTG suites that are both younger and older than the major mafic magmatic event (Abbott 1996; Wyman and Hollings 2015). Abbott (1996) also infers that higher recycling rates of Archean oceanic lithosphere implies interaction between a mid ocean ridge and a subduction setting must have been more common during Archean than in Phanerozoic. Interaction between mantle plumes and mid ocean ridges in a subduction setting are much less common during Phanerozoic. Seismic velocity maps (Zhang and Tanimoto 1992) and geochemical evidences (Bourdon *et al.* 1996; Douglass and Schilling 1999; Liu *et al.* 2017), however, show that ridge–hotspot interaction is not that uncommon in the Phanerozoic eon. Interaction of a mid ocean ridge and a subduction zone is encountered in the subduction of Chile oceanic ridge beneath the continental plate north of the Taitao peninsula (Herron *et al.* 1981; Lagabrielle *et al.* 1994; Le Moigne *et al.* 1996; Karsten *et al.* 1996; Guivel *et al.* 2003; Anma *et al.* 2009).

The Sargur ultramafic rocks are extensively found associated with spinifex-textured komatiites and pillowed tholeiitic basalts with the intrusive peridotites positioned as narrow belts tucked within the TTG complexes in the western Dharwar craton. Assuming limited mobility of incompatible elements, the Th/Yb *vs.* Nb/Yb diagram after Pearce (2008) (figure 11) shows that the ultramafic–mafic rocks of the greenstone belts studied plot slightly away from the MORB–OIB array. The sources for the magmas that produced these rocks were significantly depleted and therefore a plume-type origin for the sources similar to those in OIBs is doubtful. The trajectory of the spread of the sample points away from the array in the plot is similar to crustally contaminated MORB-type (Pearce 2008) with enrichment of trace elements ascribed to assimilation–fractional crystallization processes. The trend shown by the scatter of points in figure 11 can be explained by the interaction of NMORB-type mantle influenced by a plume in a subduction-type setting. This geochemical signature, coupled with the absence of subduction-related calc-alkaline rocks in the vicinity of the ultramafic rocks of the greenstone belts of Sargur affinity, does not support a simple plume–arc interaction model proposed for their emplacement in the WDC (Jayananda *et al.* 2008; Mukherjee *et al.* 2012). Instead, it is proposed that based on the NMORB–EMORB like geochemical signature, the probable tectonic setting for the emplacement of the ultramafic–mafic intrusive and extrusive rocks could have been a subducting mid-oceanic ridge where an upwelling plume-modified mantle underwent decompression melting. The subduction was incomplete due to steeper geothermal gradient and shallow descending of the lithosphere,

squeezing out the mantle wedge, while internal differentiation of the pooled melts developed the layered intrusive structure. The contamination of the parent melts by assimilation-fractional crystallization processes could have been effectuated by the ensuing crustal melts that eventually gave rise to granitoid intrusive rocks or by interaction with the pre-existing lithosphere. Plume-lithosphere interaction as a source of layered intrusions has also been suggested for the Windimurra Igneous Complex in the Yilgarn craton (Nebel *et al.* 2013). From the present geochemical study, it is therefore suggested that the studied greenstone belts of Sargur Group, particularly NGB, were emplaced in a mid-oceanic ridge that was suitably modified by a rising mantle plume and this setting forestalled its subduction at a convergent margin.

Petrographic study of the samples collected from the layered igneous complex of NGB does not show any significant grain size variation with respect to the modally layered rock units, though cumulous textured peridotites are found sparingly at the base of the exposed rock units. Naslund and McBirney (1996) have discussed about the processes or mechanisms that are primarily responsible for the development of layering. Naslund and McBirney (1996) showed that though gravity settling is commonly considered to be the dominant mechanism for the mechanical sorting of magmas into modally or phase layered lithologies upon crystallization and cooling, variations in intensive parameters and kinetic factors such as pressure, oxygen fugacity, nucleation and growth rate and rate of separation of immiscible liquids can all produce layering. Therefore, development of layering may be due to fluctuations in pressure, fluctuations in oxygen fugacity, chemical migration in thermal gradients in slowly cooled magmas, as well as, variations in nucleation rate (Naslund and McBirney 1996). Presence of phase layers of dunite, peridotite, pyroxenite, hornblendite, gabbro, anorthosite and titaniferous vanadiferous magnetite in a sequential manner in NGB and the lack of significant grain size variations within the layers are indicative of gravity settling process to have been dominant in NGB rocks. However, layering may not develop in magma chambers where gravity settling due to density contrasts does not set in, possibly due to lack of variations in intensive parameters. The Cenozoic Skaergaard intrusion in East Greenland is a classic example of low-pressure closed-system fractionation in a basaltic magma chamber (Holness *et al.* 2017) where the graded layers are density-sorted with insignificant grain size sorting (Naslund and McBirney 1996). The NGB probably represents a case of layering developed during fractional crystallization in relatively shallower depths, encountered in ridge–arc interaction environments, where density contrasts would have been more pronounced. Therefore, by and large, relative to melting processes, the lower pressure fractional crystallization processes were responsible for the observed variations in elemental abundances.

7. Conclusions

1. The Al-depleted and Al-undepleted signatures obtained in the layered ultramafic–mafic complexes of Holenarsipur and Nuggihalli greenstone belts of Sargur Group exposed in the western Dharwar craton could be due to magmatic differentiation processes involving fractional crystallization. Garnet need not always have a role to impart the observed Al–Ti and Gd–Yb signatures, and fractionation of hornblende and plagioclase might give rise to similar geochemical characteristics.
2. The parental magma for the generation of ultramafic–mafic layered intrusive complex of the NGB could have been homogeneous and later differentiation processes were responsible for the heterogeneity observed in the rocks of the complex. Fractional crystallization modelling explains the observed variations in the geochemical properties of the different rock types of HGB and NGB.
3. Differences in the lithological association and geochemical characteristics of the ultramafic–mafic rocks of HGB and NGB can be attributed to different lithospheric thicknesses/crustal levels encountered in these belts and the differences in the degree of interaction with older crust.
4. The HGB and NGB rocks show an NMORB–EMORB-like signature and the probable geodynamic setting for their emplacement could be in a plume-modified mid-ocean ridge that was too thick and buoyant to be subducted, and the decompression-melted magma chamber developed igneous layering as the magma stalled in the lithosphere.

Acknowledgements

The authors gratefully acknowledge the support given by Mr. Nibin Tom, Superintending

Geologist, Geological Survey of India, during the field work and lengthy discussions with him. KP acknowledges the Junior Research Fellowship provided by IIT (ISM) Dhanbad. Laboratory support extended by NCESS, Thiruvananthapuram is also acknowledged. The laboratory facilities in the Department of Applied Geology, IIT(ISM), funded through DST FIST Level II project No. SR/FST/ESII-014/2012(C), are also acknowledged. Excellent inputs from an anonymous reviewer had improved the manuscript substantially.

References

Abbott D H 1996 Plumes and hotspots as sources of greenstone belts; *Lithos* **37** 113–127.

Ananta Iyer G V and Vasudev V N 1979 Geochemistry of the Archaean metavolcanic rocks of Kolar and Hutti goldfields, Karnataka, India; *J. Geol. Soc. India* **20** 419–432.

Anhaeusser C R 2001 The anatomy of an extrusive–intrusive Archaean mafic–ultramafic sequence: the Nelshoogte Schist Belt and Stolzburg Layered Ultramafic Cmplex, Barberton Greenstone Belt, South Africa; *S. Afr. J. Geol.* **104** 167–204.

Anma R, Armstrong R, Orihashi Y, Ike S, Shin K C, Kon Y, Komiya T, Ota T, Kagashima S, Shibuya T, Yamamoto S, Veloso E E, Fanning M and Herve F 2009 Are the Taitao granites formed due to subduction of the Chile Ridge? *Lithos* **113** 246–258.

Arndt N T 2008 *Komatiites*; Cambridge University Press, Cambridge, p 467.

Arndt N T, Albarede F and Nisbet E G 1997 Mafic and ultramafic magmatism; In: *Greenstone Belts* (eds) de Wit M J and Ashwal L D, Oxford University Press, New York, pp. 233–254.

Arndt N T and Jenner G A 1986 Crustally contaminated komatiites and basalts from Kambalda, Western Australia; *Chem. Geol.* **56** 229–255.

Balakrishnan S, Hanson G N and Rajamani V 1990 Pd and Nd isotope constraints on the origin of high Mg and tholeiitic amphibolites, Kolar Schist Belt, South India; *Contrib. Miner. Pet.* **107** 279–292.

Bau M 1991 Rare earth element mobility during hydrothermal and metamorphic fluid-rock interaction and the significance of the oxidation state of europium; *Chem. Geol.* **93** 219–230.

Bau M and Knittel U 1993 Significance of slab–derived partial melts and aqueous fluids for the genesis of tholeiitic and calcalkaline island–arc basalts: Evidence from Mt. Arayat, Philippines; *Chem. Geol.* **105** 233–251.

Beckinsale R D, Drury S A and Holt R W 1980 3360 Myr old gneisses from the South Indian craton; *Nature* **283** 469–470.

Beckinsale R D, Reeves-Smith G, Gale N A, Holt R L W and Thompson B 1982 Rb–Sr and Pb–Pb whole rock isochron ages and REE data for the Archean gneisses and granites, Karnataka State, South India; In: Indo–US workshop on the Precambrian of south India [abs.], National Geophysical Research Institute, Hyderabad, India, pp. 35–36.

Bhaskar Rao Y J and Drury S A 1982 Incompatible trace element geochemistry of Archean metavolcanic rocks from Bababudan volcano sedimentary belt, Karnataka; *J. Geol. Soc. India* **23** 1–23.

Bhaskar Rao Y J and Naqvi S M 1978 Geochemistry of metavolcanics from the Bababudan schist belt; A Late Archaean/Early Proterozoic volcano-sedimentary pile from India; In: *Archaean Geochemistr*, *Dev. Precamb. Geol.* (eds) Windley B F and Naqvi S M, vol. **I**, Elsevier, Amsterdam, pp. 325–328.

Bhaskar Rao Y J, Naha K, Srinivasan R and Gopalan K 1991 Geology, geochemistry and geochronology of the Archaean peninsular gneiss around Gorur, Hassan District, Karnataka, India; *Proc. Indian Acad. Sci. (Earth Planet. Sci.)* **100** 399–412.

Bhaskar Rao Y J, Kumar A, Vrevsky A B, Srinivasan R and Anantha Iyer G V 2000 Sm–Nd ages of two meta-anorthosite complexes around Holenarsipur: Constraints on the antiquity of Archean supracrustal rocks of the Dharwar craton; *Proc. Indian Acad. Sci. (Earth Planet. Sci.)* **109** 57–65.

Bhaskar Rao Y J, Sivaraman T V, Pantulu C V C, Gopalan K and Naqvi S M 1992 Ages of late Archaean metavolcanics and granites, Dharwar craton: Evidence for early Proterozoic thermo–tectonic events; *Precambrian Res.* **38** 246–270.

Bidyananda M, Deomurari M P and Goswami J N 2003 ^{207}Pb–^{206}Pb ages of zircons from the Nuggihalli schist belt, Dharwar craton, southern India; *Curr. Sci.* **85** 1482–1485.

Bouhallier H, Choukroune P and Ballevre M 1993 Diapirism, bulk homogeneous shortening and transcurrent shearing in the Archaean Dharwar craton: The Holenarsipur area, southern India; *Precambrian Res.* **63** 43–58.

Bourdon B, Langmuir C H and Zindler A 1996 Ridge-hotspot interaction along the Mid-Atlantic Ridge between 37°30′ and 40°30′N: The U–Th disequilibrium evidence; *Earth Planet. Sci. Lett.* **142** 175–189.

Brown P E, Tocher F E and Chambers A D 1982 Amphiboles in the lilloise intrusion, East Greenland; *Miner. Mag.* **45** 47–54.

Buhl D, Grauert B and Raith M 1983 U–Pb zircon dating of Archaean rocks from the South Indian Craton: Results from the amphibolite to granulite facies transition zone at Kabbal quarry, southern Karnataka; *Fortschr. Miner.* **61** 43–45.

Chadwick B, Ramakrishnan M, Vasudev V and Viswanatha M N 1989 Facies distributions and structure of Dharwar volcanosedimentary basin: Evidence of late Archaean transpression in southern India; *J. Geol. Soc. Lond.* **146** 825–834.

Chadwick B, Ramakrishnan M and Viswanatha M N 1981 Structural and metamorphic relations between Sargur and Dharwar supracrustal rocks and peninsular gneiss in central Karnataka; *J. Geol. Soc. India* **22** 557–569.

Chadwick B, Ramakrishnan M and Viswanatha M N 1985a Bababudan—a late Archaean intra-cratonic volcano-sedimentary basin, Karnataka, southern India. Part I: Stratigraphy and basin development; *J. Geol. Soc. India* **26** 769–801.

Chadwick B, Ramakrishnan M and Viswanatha M N 1985b Bababudan—A late Archaean intra-cratonic volcano-sedimentary basin, Karnataka, southern India. Part II: Structure; *J. Geol. Soc. India* **26** 802–821.

Chadwick B, Ramakrishnan M, Viswanatha M N and Murthy V S 1978 Structural studies in the Archaean Sargur and Dharwar supracrustal rocks of the Karnataka craton; *J. Geol. Soc. India* **19** 531–549.

Chadwick B, Vasudev V N and Hegde G V 2000 The Dharwar craton, southern India, interpreted as the result of Late Archaean oblique convergence; *Precambrian Res.* **99** 91–111.

Chardon D, Jayananda M and Peucat J–J 2011 Lateral constrictional flow of hot orogenic crust: Insights from the Neoarchean of South India, geological and geophysical implications for orogenic plateaux; *Geochem. Geophys. Geosyst.* **12** Q02005, http://dx.doi.org/10.1029/2010GC003398.

Chardon D, Peucat J-J, Jayananda M, Choukroune P and Fanning C M 2002 Archean granite–greenstone tectonics at Kolar (South India): Interplay of diapirism, bulk inhomogeneous contraction during juvenile accretion; *Tectonics* **32** 1029–1047.

Chavagnac V 2004 A geochemical and Nd isotopic study of Barberton komatiites (South Africa): Implication for the Archean mantle; *Lithos* **75** 253–281.

Compston W, Williams I S, Campbell I H and Gresham J J 1986 Zircon xenocrysts from the Kambalda volcanics: Age constraints and direct evidence for older continental crust below the Kambalda–Norseman greenstones; *Earth Planet. Sci. Lett.* **76** 299–311.

Corgne A, Liebske C, Wood B J, Rubie D C and Frost D J 2005 Silicate perovskite-melt partitioning of trace elements and geochemical signature of a deep perovskitic reservoir; *Geochim. Cosmochim. Acta* **69** 485–496.

Das Sharma S, Srinivasan R, Ahmad S M and Patil D J 1994 Carbon and oxygen isotopic compositions of the regionally metamorphosed Archaean carbonate rocks of the Dharwar craton: A preliminary appraisal; *Curr. Sci.* **66** 857–860.

de Wit M J, Roering C and Hart R J 1992 Formation of an Archaean continent; *Nature* **357** 553–562.

Douglass J and Schilling J–G 1999 Plume–ridge interactions of the Discovery and Shona mantle plumes with the southern Mid Atlantic Ridge (40°–55°S); *J. Geophys. Res.* **104** 2941–2962.

Drury S A 1981 Geochemistry of Archean metavolcanic rocks from Kudremukh area, Karnataka; *J. Geol. Soc. India* **22** 405–416.

Drury S A 1982 Geochemistry of Archaean metavolcanic rocks from the Holenarsipur and Shigegudda volcano-sedimentary belts of Karnataka, south India; *Precambrian Res.* **19** 119–139.

Drury S A 1983 The petrogenesis and setting of Archaean volcanics from Karnataka state, south India; *Geochim. Cosmochim. Acta* **47** 317–329.

Drury S A, Harris N B W, Holt R W, Reeves-Smith G J and Wightman R T 1984 Precambrian tectonics and crustal evolution in south India; *J. Geol.* **92** 3–20.

Drury S A, Van Calsteren P C and Reeves–Smith G J 1987 Sm–Nd isotopic data from Archaean metavolcanic rocks at Holenarsipur, south India; *J. Geol.* **95** 837–843.

Elliott T R, Hawkesworth C J and Gronvold K 1991 Dynamic melting of Iceland plume; *Nature* **351** 106–201.

Falloon T J, Green D H, Danyushevsky L V and McNeill A W 2008 The composition of near-solidus partial melts of fertile peridotite at 1 and 1.5 GPa: Implications for the petrogenesis of MORB; *J. Pet.* **49** 591–613.

Fan J and Kerrich R 1997 Geochemical characteristics of aluminium depleted and undepleted komatiites and HREE-enriched low-Ti tholeiites, western Abitibi greenstone belt: A heterogeneous mantle plume-convergent margin environment; *Geochim. Cosmochim. Acta* **61** 4723–4744.

Fitton J G, Saunders A D, Norry M J, Hardarson B S and Taylor R N 1997 Thermal and chemical structure of the Iceland plume; *Earth Planet. Sci. Lett.* **153** 197–208.

Fryer B J, Kerrich R, Hutchinson R W, Peirce M G and Rogers D S 1979 Archaean precious–metal hydrothermal systems, Dome Mine, Abitibi Greenstone belt. I: Patterns of alteration and metal distribution; *Can. J. Earth Sci.* **16** 421–439.

Green D H 1975 Genesis of Archean peridotitic magmas and constraints on Archean geothermal gradients and tectonics; *J. Geol. Soc. Am.* **3** 15–18.

Grove T L and Parman S W 2004 Thermal evolution of the Earth as recorded by komatiites; *Earth Planet. Sci. Lett.* **219** 173–187.

Groves D I, Lesher C M and Gee R D 1984 Tectonic setting of the sulphide nickel deposits of the Western Australian Shield; In: *Sulphide Deposits in Mafic and Ultramafic Rocks* (eds) Buchanan D L and Jones M J, Institution of Mining and Metallurgy, London, pp. 1–13.

Gruau G, Tourpin S, Fourcade S and Blais S 1992 Loss of isotopic (Nd, O) and chemical (REE) memory during metamorphism of komatiites: New evidence from eastern Finland; *Contrib. Miner. Pet.* **112** 66–82.

Guivel C, Lagabrielle Y, Bourgois J, Martin H, Arnaud N, Fourcade S, Cotten J and Maury R C 2003 Very shallow melting of oceanic crust during spreading ridge subduction: Origin of near-trench Quaternary volcanism at the Chile Triple Junction; *J. Geophys. Res.* **108** 2345, https://doi.org/10.1029/2002jb002119.

Gupta S, Rai S S, Prakasam K S, Srinagesh D, Chadha R K, Priestley K and Gaur V K 2003 First evidence for anomalous thick crust beneath mid-Archean western Dharwar craton; *Curr. Sci.* **84** 1219–1226.

Herron E M, Cande S C and Hall B R 1981 An active spreading center collides with a subduction zone: A geophysical survey of the Chile Margin triple junction; *J. Geol. Soc. Am. Memoir.* **154** 683–701.

Herzberg C 1992 Depth and degree of melting of komatiites; *J. Geophys. Res.* **97** 4521–4540.

Herzberg C 1999 Phase equilibrium constraints on the formation of cratonic mantle; In: *Mantle Petrology: Field observations and high pressure experimentation. A tribute to Francis R (Joe) Boyd* (eds) Fei Y, Bertka C and Mysen B O, *Geochem. Soc. Spec. Publ.* **6** 241–257.

Herzberg C and O'Hara M J 2002 Plume-associated ultramafic magmas of Phanerozoic age; *J. Pet.* **43** 1857–1883.

Herzberg C and Zhang J 1996 Melting experiments on anhydrous KLB–1: Compositions of magmas in the upper mantle and transition zone; *J. Geophys. Res.* **101** 8271–8295.

Hokada T, Horie K, Satish-Kumar M, Ueno Y, Nasheeth A, Mishima K and Shiraishi K 2012 An appraisal of Archaean supracrustal sequences in Chitradurga schist belt, western Dharwar craton, southern India; *Precambrian Res.* **227** 99–119.

Hollings P, Wyman D A and Kerrich R 1999 Komatiite–basalt–rhyolite volcanic associations in Northern Superior Province greenstone belts: Significance of plume–arc interaction in the generation of the proto continental Superior Province; *Lithos* **46** 137–161.

Holness M B, Nielsen T F D and Tegner C 2017 The Skaergaard Intrusion of East Greenland: Paradigms, problems and new perspectives; *Elements* **14** 391–396.

Huppert H E, Sparks R S J, Turner J S and Arndt N T 1984 Emplacement and cooling of komatiite lavas; *Nature* **309** 19–22.

Hussain S M and Naqvi S M 1983 Geological, geophysical and geochemical studies over the Holenarsipur schist belt, Dharwar craton, India; In: *Precambrian of South India* (eds) Naqvi S M and Rogers J J W, *J. Geol. Soc. India Memoir* **4** pp. 73–95.

Hynes A 1980 Carbonatization and mobility of Ti, Y and Zr in Ascot formation, S.E. Quebec; *Contrib. Miner. Pet.* **75** 79–87.

Jafri S H, Subba Rao D V, Ahmad S M and Mathur R 1997 Spinifex textured peridotitic komatiites from Nuggihalli and Holenarsipur schist belts, Karnataka; *J. Geol. Soc. India* **49** 33–38.

Jayananda M, Chardon D, Peucat J-J and Capdevila R 2006 2.61 Ga potassic granites and crustal reworking in the western Dharwar craton, southern India: Tectonic, geochronologic and geochemical constraints; *Precambrian Res.* **150** 1–26.

Jayananda M, Chardon D, Peucat J-J, Tushipokla and Fanning C M 2015 Paleo- to Mesoarchean TTG accretion and continental growth in the western Dharwar craton, southern India: Constraints from SHRIMP U–Pb zircon geochronology, whole-rock geochemistry and Nd–Sr isotopes; *Precambrian Res.* **268** 295–322.

Jayananda M, Kano T, Peucat J-J and Channabasappa S 2008 3.35 Ga komatiite volcanism in the western Dharwar craton, southern India: Constraints from Nd isotopes and whole rock geochemistry; *Precambrian Res.* **162** 160–179.

Jayananda M, Moyen J-F, Martin H, Peucat J-J, Auvray B and Mahabaleswar B 2000 Late Archean (2550–2520 Ma) juvenile magmatism in the Eastern Dharwar craton, southern India: Constraints from geochronology, Nd–Sr isotopes and whole rock geochemistry; *Precambrian Res.* **99** 225–254.

Jayananda M, Peucat J-J, Chardon D, Krishna Rao B, Fanning C M and Corfu F 2013 Neoarchean greenstone volcanism and continental growth, Dharwar craton, southern India: Constraints from SIMS U–Pb zircon geochronology and Nd isotopes; *Precambrian Res.* **227** 55–76.

Jensen L S 1976 A new method of classifying alkali volcanic rocks; *Ont. Div. Miner. Misc. Paper* **66** 22.

Jochum K P, Arndt N T and Hofmann A W 1991 Nb–Th–La in komatiies and basalts: Constraints on komatiite petrogenesis and mantle evolution; *Earth Planet. Sci. Lett.* **107** 272–289.

Karsten J L, Klein E M and Sherman S B 1996 Subduction zone geochemical characteristics in ocean ridge basalts from the southern Chile Ridge: Implications of modern ridge subduction systems for the Archean; *Lithos* **37** 143–161.

Kato Y, Kawakami T, Kano T, Kunugiza K and Swamy N S 1996 Rare-earth element geochemistry of banded iron formations and associated amphibolite from the Sargur belts, South India; *J. Southeast Asian Earth Sci.* **14** 161–164.

Keiding J K, Trumbull R B, Veksler I V and Jerram D A 2011 On the significance of ultra-magnesian olivines in basaltic rocks; *Geology* **39** 1095–1098.

Kerr A C, Marriner G F, Arndt N T, Tarney J, Nivia A, Saunders A D and Duncan R A 1996 The petrogenesis of Gorgona komatiites, picrites and basalts: New field, petrographic and geochemical constraints; *Lithos* **37** 245–260.

Kerr A C, Saunders A D, Tarney J, Berry N and Hards V L 1995 Depleted mantle plume geochemical signatures; no paradox for plume theories; *Geology* **23** 843–846.

Kerrich R, Polat A, Wyman D and Hollings P 1999 Trace element systematics of Mg- to Fe-tholeiitic basalt. Suites of the Superior Province: Implications for Archean mantle reservoirs and greenstone belt genesis; *Lithos* **46** 163–187.

Kerrich R and Xie Q 2002 Compositional recycling structure of an Archean super-plume: Nb–Th–U–LREE systematics of Archean komatiites and basalts revisited; *Contrib. Miner. Pet.* **142** 476–484.

King R W and Kerrich R 1987 Fluorapatite fenitization and gold enrichment in sheeted trondhjemites within the Destor–Porcupine fault zone, Taylor Township, Ontario; *Can. J. Earth Sci.* **24** 479–502.

Kroner A, Anhaeusser C R, Hoffmann J E, Wong J, Geng H, Hegner E, Xie H, Yang J and Liu D 2016 Chronology of the oldest supracrustal sequences in the Palaeoarchaean Barberton Greenstone Belt, South Africa and Swaziland; *Precambrian Res.* **279** 123–143.

Kumar A, Bhaskar Rao Y J, Sivaraman T V and Gopalan K 1996 Sm–Nd ages of Archaean metavolcanics of the Dharwar craton, South India; *Precambrian Res.* **80** 205–216.

Kunugiza K, Kato Y, Kano T, Takaba Y, Kuruma I and Sohma T 1996 An Archaean tectonic model of the Dharwar craton, southern India: The origin of the Holenarsipur greenstone belt (Hussan district, Karnataka) and reinterpretation of the Sargur–Dharwar relationship; *J. Southeast Asian Earth Sci.* **14** 149–160.

Lagabrielle Y, Moigne Le J, Maury R C, Gotten J and Bourgois J 1994 Volcanic record of the subduction of an active spreading ridge, Taitao peninsula (southern Chile); *Geology* **22** 515–518.

Lahaye Y and Arndt N 1996 Alteration of a komatiites flow from Alexo, Ontario, Canada; *J. Pet.* **37** 1261–1284.

Lahaye Y, Arndt N, Byerly G, Chauvel C, Fourcade S and Gruau G 1995 The influence of alteration on the trace-element and Nd isotopic compositions of komatiites; *Chem. Geol.* **126** 43–64.

Lesher C M and Arndt N T 1995 REE and Nd isotope geochemistry, petrogenesis and volcanic evolution of contaminated komatiites at Kambalda, Western Australia; *Lithos* **34** 127–158.

Liu X, Xiao W, Xu J, Castillo P R and Shi Y 2017 Geochemical signature and rock associations of ocean ridge–subduction: Evidence from the Karamaili Paleo–Asian ophiolite in east Junggar, NW China; *Gondwana Res.* **48** 34–49.

Ludden J N, Daigneault R, Robert F and Taylor R P 1984 Trace element mobility in alteration zones associated with Archaean Au lode deposits; *Econ. Geol.* **79** 1131–1141.

Manikyamba C and Naqvi S M 1997 Late Archaean mantle fertility: Constraints from metavolcanics of the Sandur schist belt, India; *Gondwana Res.* **1** 69–89.

Manikyamba C, Naqvi S M, Rao D V S, Mohan M R, Khanna T C, Rao T G and Reddy G L N 2005 Boninites from the Neoarchaean Gadwal Greenstone belt, eastern Dharwar Craton, India: Implications for Archaean subduction processes; *Earth Planet. Sci. Lett.* **230** 65–83.

Maya J M, Bhutani R, Balakrishnan S and Rajee Sandya S 2016 Petrogenesis of 3.15 Ga old Banasandra komatiites

from the Dharwar craton, India: Implications for early mantle heterogeneity; *Geosci. Front.* **8** 467–481.

McCulloch M T and Black L P 1984 Sm–Nd isotopic systematics of Enderby Land granulites and evidence for the redistribution of Sm and Nd during metamorphism; *Earth Planet. Sci. Lett.* **71** 46–58.

Meen J K, Rogers J J W and Fullagar P D 1992 Lead isotope composition in the western Dharwar craton, southern India: Evidence for distinct middle Archaean terraines in the late Archaean craton; *Geochim. Cosmochim. Acta* **56** 2455–2470.

Moigne Le J, Lagabrielle Y, Whitechurch H, Girardeau J, Bourgois J and Maury R C 1996 Petrology and geochemistry of the ophiolitic and volcanic suites of the Taitao peninsula—Chile triple junction area; *J. South Am. Earth Sci.* **9** 43–58.

Monrad J R 1983 Evolution of sialic terranes in the vicinity of the Holenarasipur belt, Hassan district, Karnataka, India; *Geol. Soc. India Mem.* **4** 343–364.

Mukherjee R, Mondal S K, Frei R, Rosing M T, Waight T E, Zhong H and Kumar G R R 2012 The 3.1 Ga Nuggihalli chromite deposits, Western Dharwar craton (India): Geochemical and isotopic constraints on mantle sources, crustal evolution and implications for supercontinent formation and ore mineralization; *Lithos* **155** 392–409.

Mukherjee R, Mondal S K, Rosing M T and Frei R 2010 Compositional variations in the Mesoarchean chromites of the Nuggihalli schist belt, Western Dharwar craton (India): Potential parental melts and implications for tectonic setting; *Contrib. Miner. Pet.* **160** 865–885.

Murphy J B and Hynes A J 1986 Contrasting secondary mobility of Ti, P, Zr, Nb, and Y in two metabasaltic suites in the Appalachians; *Can. J. Earth Sci.* **23** 1138–1144.

Naha K, Srinivasan R, Gopalan K, Pantulu G V C, Subba Rao M V, Vrevsky A B and Bogomolov Y E S 1993 The nature of the basement in the Archaean Dharwar craton of southern India and the age of the peninsular gneiss; *Proc. Indian Acad. Sci. (Earth Planet. Sci.)* **102** 547–565.

Naha K, Srinivasan R and Jayaram S 1991 Sedimentational, structural and migmatitic history of the Archaean Dharwar tectonic province, southern India; *Proc. Indian Acad. Sci. (Earth Planet. Sci.)* **100** 413–433.

Naqvi S M 1981 The oldest supracrustals of the Dharwar craton, India; *J. Geol. Soc. India* **23** 458–469.

Naqvi S M 2005 *Geology and evolution of the Indian Plate from Hadean to Holocene (4.0 Ga–4.0 Ka)*; Capital Books, New Delhi, 450p.

Naqvi S M and Hussain S M 1973 Relation between trace and major element composition of Chitradurg metabasalts, Mysore, India, and the Archaean mantle; *Chem. Geol.* **11** 17–30.

Naqvi S M, Khan R M K, Manikyamba C, Ram Mohan M and Khanna T C 2006 Geochemistry of the Neoarchaean high-Mg basalts, boninites and adakites from the Kushtagi–Hungund greenstone belt of the Eastern Dharwar Craton (EDC): Implications for the tectonic setting; *J. Asian Earth Sci.* **27** 25–44.

Naqvi S M, Manikyamba C, Gnaneswar Rao T, Subba Rao D V, Ram Mohan M and Srinivasa Sarma 2002 Geochemical and isotopic constraints of Neoarchaean fossil plume for evolution of volcanic rocks of Sandur greenstone belt, India; *J. Geol. Soc. India* **60** 27–56.

Naqvi S M and Prathap J G R 2007 Geochemistry of adakites from Neoarchaean active continental margin of Shimoga schist belt, Western Dharwar Craton, India: Implications for the genesis of TTG; *Precambrian Res.* **156** 32–54.

Naqvi S M and Rogers J J W 1987 *Precambrian geology of India*; Oxford University Press, New York, p. 223.

Naqvi S M, Viswanatha S and Viviswanatha M N 1978 Geology and geochemistry of the Holenarsipur schist belt and its place in the evolutionary history of the Indian peninsula; In: *Archean Geochemistry* (eds) Windley B F and Naqvi S M, Elsevier, Amsterdam, pp. 109–126.

Naslund H R and McBirney A 1996 Mechanisms of formation of igneous layering; In: *Layered Intrusions* (ed) Cawthorn R G, Elsevier Science B.V., Amsterdam, pp. 1–43.

Nebel O, Arculus R J, Ivanic T J and Nebel-Jecobsaen Y J 2013 Lu–Hf isotopic memory of plume–lithosphere interaction in the source of layered mafic intrusions, Windimurra Igneous Complex, Yilgarn Craton, Australia; *Earth Planet. Sci. Lett.* **380** 151–161.

Nutman A P, Chadwick B, Krishna Rao B and Vasudev V N 1996 SHRIMP U–Pb ages of acid volcanic rocks in the Chitradurga and Sandur Groups and granites adjacent to Sandur schist belt; *J. Geol. Soc. India* **47** 153–161.

Nutman A P, Chadwick B, Ramakrishnan M and Viswanatha M N 1992 SHRIMP U–Pb ages of detrital zircon in Sargur supracrustal rocks in western Karnataka, southern India; *J. Geol. Soc. India* **39** 367–374.

Ohtani E 1984 Generation of komatiite magma and gravitational differentiation in the deep upper mantle; *Earth Planet. Sci. Lett.* **67** 261–272.

Ohtani E 1990 Majorite fractionation and genesis of komatiites in the deep mantle; *Precambrian Res.* **48** 195–202.

Ohtani E, Kawabe I, Moriyama J and Nagata Y 1989 Partitioning of elements between majorite garnet and melt and implications for petrogenesis of komatiite; *Contrib. Miner. Pet.* **103** 263–269.

Ordóñez-Calderón J C, Polat A, Fryer B, Gagnon J E, Raith J G and Appel P W U 2008 Evidence for HFSE and REE mobility during calc-silicate metasomatism, Mesoarchean (∼3075 Ma) Ivisaartoq greenstone belt, southern West Greenland; *Precambrian Res.* **161** 317–340.

Page N J and Zientek M L 1987 Composition of primary postcumulus amphibole and phlogopite within an olivine cumulate in the stillwater complex, Montana; *US Geol. Surv. Bull.* **1674-A** 35.

Patra K, Anand R, Balakrishnan S, Dash J K and Tom N G 2016 Constraints on the evolution of the mafic–ultramafic rock suites of selected Mesoarchean greenstone belts of western Dharwar craton, southern India; Goldschmidt 2016, 26 June–1 July, Yokohama, Japan.

Pearce J A 2008 Geochemical fingerprinting of oceanic basalts with applications to ophiolite classification and the search for Archean oceanic crust; *Lithos* **100** 14–48.

Peucat J–J, Bouhallier H, Fanning C M and Jayananda M 1995 Age of Holenarsipur schist belt, relationships with the surrounding gneisses (Karnataka, south India); *J. Geol.* **103** 701–710.

Peucat J-J, Mahabaleswar B and Jayananda M 1993 Age of younger tonalitic Magmatism and granulite metamorphism in the south Indian transition zone (Krishnagiri area): Comparison with older peninsular gneisses from Hassan–Gorur area; *J. Metamorph. Geol.* **11** 879–999.

Peucat J J, Vidal P, Bernard-Griffiths J and Condie K C 1987 Sr, Nd and Pb systems across the amphibolite to granulite facies transition in southern India; *Terra Cognita* **7** 333.

Peucat J J, Vidal P, Bernard-Griffiths J and Condie K C 1989 Sr, Nd and Pb isotopic systematics in the Archean low- to high-grade transition zone of southern India: Syn-accretion *vs.* post-accretion granulites; *J. Geol.* **97** 537–550.

Polat A and Kerrich R 2000 Archean greenstone belt magmatism and the continental growth–mantle evolution connection: Constraints from Th–Nb–U–LREE systematics of the 2.7 Ga Wawa subprovince, Superior Province, Canada; *Earth Planet. Sci. Lett.* **175** 41–54.

Polat A, Kerrich R and Wyman D A 1998 The late Archean Schreiber–Hemlo and White River–Dayohessarah greenstone belts, Superior Province: Collages of oceanic plateaus, oceanic arcs, and subduction–accretion complexes; *Tectonophys.* **289** 295–326.

Polat A, Kerrich R and Wyman D A 1999 Geochemical diversity in oceanic komatiites and basalts from the late Archean Wawa greenstone belts, Superior Province, Canada: Trace element and Nd isotope evidence for a heterogeneous mantle; *Precambrian Res.* **94** 139–173.

Polat A, Longstaffe F J and Frei R 2018 An overview of anorthosite-bearing layered intrusions in the Archaean craton of southern West Greenland and the Superior Province of Canada: Implications for Archaean tectonics and the origin of megacrystic plagioclase; *Geodin. Acta* **30** 84–99.

Polat A, Fryer B J, Samson I M, Weisener C, Appel P W U, Frei R and Windley B F 2012 Geochemistry of ultramafic rocks and hornblendite veins in the Fiskenæsset layered anorthosite complex, SW Greenland: Evidence for hydrous upper mantle in the Archean; *Precambrian Res.* **214–215** 124–153.

Puchtel I S, Hofmann A W, Amelin Y W, Grabe-Schonberg C-D, Samsonov A V and Shchipansky A A 1999 Sumozero–Kenozero greenstone belt, SE Baltic Shield: Isotope and trace element constraints; *Geochim. Cosmochim. Acta* **63** 3579–3595.

Radhakrishna B P and Naqvi S M 1986 Precambrian continental crust of India and its evolution; *J. Geol.* **94** 145–166.

Radhakrishna B P and Vaidyanadhan R 1997 Geology of Karnataka; *Geol. Soc. India Banglore* 49–73.

Rai S S, Borah K, Das R, Gupta S, Srivastava S, Prakasam K S, Sivaram K, Kumar S and Meena R 2013 The south India Precambrian crust and shallow lithospheric mantle: Initial results from the India Deep Earth Imaging Experiment (INDEX); *J. Earth Syst. Sci.* **122** 1435–1453.

Ramakrishnan M, Kroner A and Vankata Dasu S P 1994 Mid–Archean zircon age of Sargur Group by single grain zircon dating and geochemical evidence from clastic origin of metaquartzite from JC Pura greenstone belt, Karnataka; *J. Geol. Soc. India* **29** 471–482.

Ramakrishnan M and Viswanatha M N 1981 Holenarsipur belt; In: *Early Precambrian Supracrustals of Southern Karnataka* (eds) J Swami Nath and M Ramakrishnan, *Geol. Surv. India Memoir* **112** 115–141.

Revillon S, Arndt N T, Chauvel C and Hallot E 2000 Geochemical study of ultramafic volcanic and plutonic rocks from Gorgona Island, Colombia: The plumbing system of an oceanic plateau; *J. Pet.* **41** 1127–1153.

Robin–Popieul C C M, Arndt N T, Chauvel C, Byerly G R, Sobolev A V and Wilson A 2012 A new model for Berberton komatiites: Deep critical melting with high melt retention; *J. Pet.* **53** 2191–2229.

Rogers J J W 1996 A history of continents in the past three billion years; *J. Geol.* **104** 91–107.

Rollinson H 1993 *Using Geochemical Data: Evaluation, Presentation, Interpretation*; Pearson Education Limited, Harlow, p. 352.

Rollinson H R, Windley B F and Ramakrishnan M 1981 Contrasting high and intermediate pressures of metamorphism in the Archean Sargur Schists of southern India; *Contrib. Miner. Pet.* **76** 420–429.

Rubin J N, Henry C D and Price J C 1988 Hydrothermal zircons and zircon overgrowths, Sierra Blanca Peaks, Texas; *Am. Miner.* **74** 865–869.

Rubin J N, Henry C D and Price J C 1993 The mobility of zirconium and other 'immobile' elements during hydrothermal alteration; *Chem. Geol.* **110** 29–47.

Sappin A-A, Houle M G, Lesher C M, McNicoll V, Vaillancourt C and Kamber B S 2016 Age constraints and geochemical evolution of the Neoarchean mafic–ultramafic Wabassi Intrusive Complex in the Miminiska–Fort Hope greenstone belt, Superior Province, Canada; *Precambrian Res.* **286** 101–125.

Sarma D S, Fletcher I R, Rasmussen B, Mc Naughton N J, Ram Mohan M and Groves D I 2011 Archaean gold mineralisation synchronous with late cratonisation of the western Dharwar Craton, India and xenotime in gold deposits; *Miner. Depos.* **46** 273–288.

Saunders A D, Tarney J, Kerr A C and Kent R W 1996 The formation and fate of large oceanic igneous provinces; *Lithos* **37** 81–95.

Schau M 1977 Komatiites and quartzites in the Archaean Price Albert Group; In: *Volcanic Regimes in Canada* (eds) Baragar W R A, Coleman L C and Hall J M, *Geol. Association Canada, Spl. paper* **16** pp. 341–354.

Sobolev A V, Asafov E V, Gurenko A A, Arndt N T, Batanova V G, Portnyagin M V, Garbe–Schonberg D and Krasheninnikov S P 2016 Komatiites reveal a hydrous Archaean deep-mantle reservoir; *Nature* **531** 628.

Sossi P A, Eggins S M, Nesbitt R W, Nebel O, Hergt J M, Campbell I H, O'Neill H St C, Van Kranendonk M and Rhodri Devies D 2016 Petrogenesis and geochemistry of Komatiites; *J. Pet.* **57** 147–184.

Srikantappa C, Raith M and Ackermand D 1985 High–grade regional metamorphism of ultramafic and mafic rocks from the Archaean Sargur terrane, Karnataka, south India; *Precambrian Res.* **30** 189–219.

Srikantia S V and Rao M S 1990 Unusual concentric structure in komatiite of Kibbanahalli Arm of Chitradurga supracrustal belt near Banasandra, Karnataka; *J. Geol. Soc. India* **36** 424–429.

Srikantia S V and Venkataramana P 1989 The Archaean komatiites of Nagamangala supracrustal belt, Karnataka; *J. Geol. Soc. India* **33** 210–214.

Srinivasan R 1988 Present status of the Sargur group of the Archean Dharwar craton, south India; *Indian J. Geol.* **60** 57–78.

Storey M, Mahoney J J, Kroenke L W and Saunders A D 1991 Are oceanic plateaus sites of komatiite formation? *Geology* **19** 376–379.

Swami Nath J and Ramakrishnan M 1981 Early Precambrian supracrustals of southern Karnataka; *Mem. Geol. Surv. India* **112** 350.

Swami Nath J, Ramakrishnan M and Viswanatha M N 1976 Dharwar stratigraphic model and Karnataka craton evolution; *Rec. Geol. Surv. India* **107** 149–175.

Taura H, Yurimoto H, Kato T and Sueno S 2001 Trace element partitioning between silicate perovskites and ultracalcic melt; *Phys. Earth Planet. Inter.* **124** 25–32.

Taylor P N, Chadwick B, Moorbath S, Ramakrishnan M and Viswanatha M N 1984 Petrography, chemistry and isotopic ages of peninsular gneiss, Dharwar acid volcanic rocks and the Chitradurga granite with special reference to the late Archean evolution of the Karnataka craton, southern India; *Precambrian Res.* **23** 349–375.

Tourpin S, Gruau G, Blais S and Fourcade S 1991 Resetting of REE, and Nd and Sr isotopes during carbonitization of a komatiite flow from Finland; *Chem. Geol.* **90** 15–29.

Trendall A F, de Laeter J R, Nelson D R and Bhaskar Rao Y J 1997a Further zircon U–Pb age data for the Daginkatte Formation, Dharwar Supergroup, Karnataka craton; *J. Geol. Soc. India* **50** 25–30.

Trendall A F, de Laeter J R, Nelson D R and Mukhopadhyay D 1997b A precise U–Pb age for the base of Mulaingiri Formation (Bababudan Group, Dharwar Supergroup) of the Karnataka craton; *J. Geol. Soc. India* **50** 161–170.

Tushipokla and Jayananda M 2013 Geochemical constraints on komatiite volcanism from Sargur Group Nagamangala greenstone belt, western Dharwar craton, southern India: Implications for Mesoarchean mantle evolution and continental growth; *Geosci. Front.* **4** 321–340.

Viljoen R P and Viljoen M J 1982 Komatiites—A historical review, In: *Komatiites* (eds) Arndt N T and Nisbet E G, George Allen and Unwin, London, pp. 5–18.

Viswanatha M N and Ramakrishnan M 1975 The pre-Dharwar supracrustal rocks of the Sargur schist complex in southern Karnataka and their tectono-metamorphic significance; *Indian Mineral.* **16** 48–65.

Viswanatha M N, Ramakrishnan M and Narayana Kutty T R 1977 Possible spinifex texture in a serpentinite from Karnataka; *J. Geol. Soc. India* **18** 194–197.

Williams D A, Kerr R C and Lesher C M 1998 Emplacement and erosion by Archean komatiite lava flows at Kambalda: Revisited; *J. Geophys. Res. Solid Earth* **103** 27,533–27,549.

Williams D A, Kerr R C, Lesher C M and Barnes S J 2002 Analytical/numerical modelling of komatiite lava emplacement and thermal erosion at Perseverance, Western Australia; *J. Volcanol. Geotherm. Res.* **110** 27–55.

Windrim D P, McCulloch M T, Chappell B W and Cameron W E 1984 Nd isotopic systematics and chemistry of Central Australian Sapphirine granulites: An example of rare earth element mobility; *Earth Planet. Sci. Lett.* **70** 27–39.

Wood S A 1990 The aqueous geochemistry of the rare earth elements and yttrium, 1. Review of available low temperature data of inorganic complexes and the inorganic speciation of natural waters; *Chem. Geol.* **82** 159–186.

Wyman D and Hollings P 2015 Long-lived mantle–plume influence on an Archean protocontinent: Geochemical evidence from the 3 Ga Lumby Lake greenstone belt, Ontario, Canada; *Geology* **26** 719–722.

Zachariah J K, Hanson G N and Rajamani V 1995 Post crystallization disturbance in the neodymium and lead isotope systems of metabaslts from the Ramagiri Schist belt, south India; *Geochim. Cosmochim. Acta* **59** 3189–3203.

Zhang J and Herzberg C 1994 Melting experiments on anhydrous peridotite KLB-1 from 5.0 to 22.5 GPa; *J. Geophys. Res.* **99** 17729–17742.

Zhang Y–S and Tanimoto T 1992 Ridges, hotspots and their interaction as observed in seismic velocity maps; *Nature* **355** 45–49.

Zhang Z, Mao J, Saunders A D, Ai Y, Li Y and Zhao L 2009 Petrogenetic modelling of three mafic–ultramafic layered intrusions in the Emeishan large igneous province, SW China, based on isotopic and bulk chemical constraints; *Lithos* **113** 369–392.

Zhou S, Polat A, Longstaffe F J, Yang K G, Fryer B J and Weisener C 2016 Formation of the Neoarchean Bad Vermilion Lake Anorthosite Complex and spatially associated granitic rocks at a convergent plate margin, Superior Province, Western Ontario, Canada; *Gondwana Res.* **33** 134–159.

Corresponding editor: N V Chalapathi Rao